Shear velocity structure in the Aegean region obtained by joint inversion of Rayleigh and Love waves

E. E. KARAGIANNI & C. B. PAPAZACHOS

Aristotle University of Thessaloniki, Geophysical Laboratory, PO Box 352-1, GR 54124 Thessaloniki, Greece (e-mail: elkarag@geo.auth.gr)

Abstract: We present a shear velocity model of the crust and uppermost mantle under the Aegean region by simultaneous inversion of Rayleigh and Love waves. The database consists of regional earthquakes recorded by portable broadband three-component digital stations that were installed for a period of 6 months in the broader Aegean region. For each epicentre–station ray path group velocity dispersion curves are measured using appropriate frequency time analysis (FTAN). The dispersion measurements for more than 600 Love wave paths have been used. We have also incorporated previous results for *c*. 700 Rayleigh wave paths for the study area. The single-path dispersion curves of both waves were inverted to regional group velocity maps for different values of period (6–32 s) via a tomographic method. The local dispersion curves of discrete grid points for both surface waves were inverted nonlinearly to construct 1D models of shear-wave velocity v. depth. In most cases the joint inversion of Rayleigh and Love waves resulted in a single model (from the multiple models compatible with the data) that could interpret both Rayleigh and Love wave data. Around 60 local dispersion curves for both Rayleigh and Love waves were finally jointly inverted. As expected, because of the complex tectonic environment of the Aegean region the results show strong lateral variations of the S-wave velocities for the crust and uppermost mantle. Our results confirm the presence of a thin crust typically less than 28–30 km in the whole Aegean Sea, which in some parts of the southern and central Aegean Sea becomes significantly thinner (20–22 km). In contrast, a large crustal thickness of about 40–45 km exists in western Greece, and the remaining part of continental Greece is characterized by a mean crustal thickness of about 35 km. A significant sub-Moho upper mantle low-velocity zone (LVLmantle) with velocities as low as 3.7 km s^{-1}, is clearly identified in the southern and central Aegean Sea, correlated with the high heat flow in the mantle wedge above the subducted slab and the related active volcanism in the region. The results obtained results are compared with independent body-wave tomographic information on the velocity structure of the study area and exhibit a generally good agreement, although significant small-scale differences are also identified.

In the present study we present a new high-resolution shear velocity model for the crust and uppermost mantle of the Aegean area obtained by the simultaneous inversion of Rayleigh and Love wave group velocities. The Aegean region (Fig. 1) lies at the convergence zone of the Eurasian and African lithospheric plates and is characterized by a complex tectonic setting. The Eastern Mediterranean plate is subducting under the Aegean, and this results in the formation of a well-defined Benioff zone (Papazachos & Comninakis 1969, 1971; Caputo *et al.* 1970; McKenzie 1970, 1978; Le Pichon & Angelier 1979). The Aegean microplate is moving at an average velocity of *c*. 35–40 mm a^{-1} towards the SW with respect to Eurasia (McKenzie 1972; Jackson 1994; Papazachos *et al.* 1998; McClusky *et al.* 2000) and is characterized by high tectonic activity, with volcanic activity (e.g. Georgalas 1962), magnetic anomalies and positive isostatic anomalies (e.g. Fleischer 1964; Vogt & Higgs 1969; Makris 1976), high heat flow (e.g. Fytikas *et al.* 1984) and high attenuation of seismic energy (e.g. Papazachos & Comninakis 1971; Hashida *et al.* 1988).

The main topographic features of tectonic origin and the local stress field of the study area are shown in Figure 1 (modified from Papazachos & Papazachou 1997). Two of the main sedimentary basins in Greece are depicted, namely the Axios basin with a maximum thickness of sediments of about 10 km (Roussos 1994), and the North. Aegean trough, with a sedimentary thickness of about 6 km (Kiriakidis 1988). In the same figure the main characteristics of the Hellenic arc, such as the volcanic arc, the sedimentary arc (Hellenides mountain range), the southern Aegean basin and the Hellenic trench, are also shown. The main zone of compression, with thrust faults that are observed along the Hellenic arc and along the western coast of northern Greece and Albania, is associated with the subduction of the Eastern Mediterranean beneath the Aegean (Papazachos & Delibasis

From: TAYMAZ, T., YILMAZ, Y. & DILEK, Y. (eds) *The Geodynamics of the Aegean and Anatolia.* Geological Society, London, Special Publications, **291**, 159–181.
DOI: 10.1144/SP291.8 0305-8719/07/$15.00

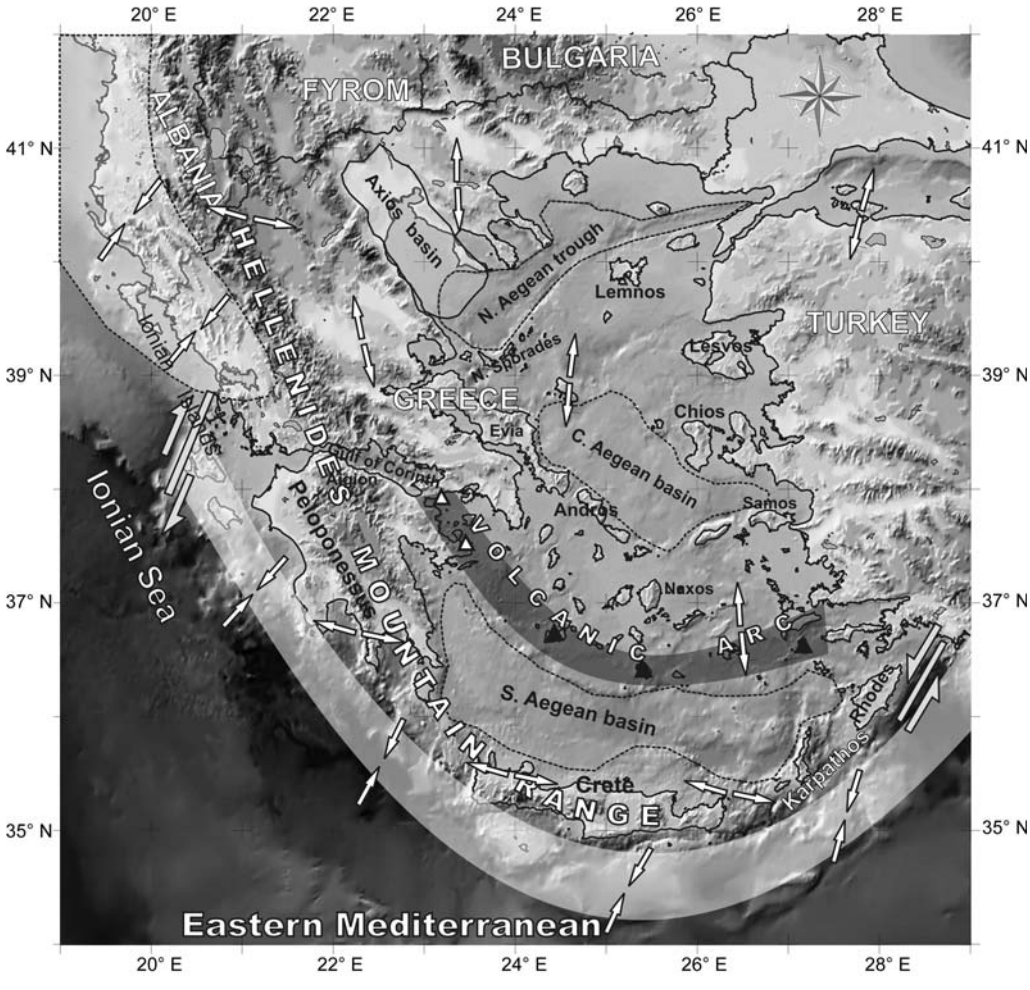

Fig. 1. Main seismotectonic features of the broader Aegean region (modified from Papazachos *et al.* 1998).

1969) and the continental–continental-type collision between the Adriatic (Apulia) microplate and the western Greek–Albanian coasts (Anderson & Jackson 1987). A dextral strike-slip zone (North Anatolian Fault; NAF) is observed in the North Anatolia–North Aegean trough (McKenzie 1970, 1972; Taymaz *et al.* 1991) and the Kefallonia area (Scordilis *et al.* 1985). The North Anatolia Fault was studied by Canitez & Toksoz (1971), who combined body- and surface-wave data and estimated the focal depth and the source parameters for earthquakes located at the fault. Later Saatcilar *et al.* (1999) mapped the active faults in the north Aegean by using reprocessed seismic reflection data, and suggested that the area is dominated by normal faults in an extensional regime, whereas for the east–central Aegean area they assumed active normal faults that instantaneously act as strike-slip faults and generate earthquakes of $M > 5.0$. The largest part of the back-arc Aegean area is dominated by normal faults with an east–west trend, suggesting north–south extension (e.g. Kurt *et al.* 1999). Finally, a narrow zone of east–west extension lies between the thrust faults of the outer Hellenic arc and the normal faults in the back-arc area, as has been identified using fault-plane solutions (e.g. Papazachos *et al.* 1984, 1998; Kiratzi *et al.* 1987), as well as by recent global positioning system (GPS) measurements (McClusky *et al.* 2000). Taymaz *et al.* (1991) used improved focal mechanisms of earthquakes constrained by P- and SH-body-wave modelling and first motions and showed that the western Aegean area is dominated by normal faults whereas the central and eastern Aegean is dominated by right-lateral strike-slip faults.

The velocity structure of the crust and upper mantle in the Aegean area has been extensively studied mainly using either body waves (usually P-waves) and partly surface-wave data. Travel times of body waves generated either by earthquakes (Panagiotopoulos 1984; Panagiotopoulos & Papazachos 1985; Plomerova *et al.* 1989; Taymaz 1996) or by explosions (Makris 1973, 1978; Delibasis *et al.* 1988; Voulgaris 1991; Bohnhoff *et al.* 2001) have been used for the study of the velocity structure under the Aegean region. An example is the work of Clement *et al.* (2004), who studied the seismicity and crustal deformation in the Gulf of Corinth by the use of seismic reflection and wide-angle reflection–refraction profiles. Their results depict the Moho discontinuity at a depth of about 40 km under the western end of the Gulf north of Aigion, which rises to a depth of about 32 km under the northern coast in the eastern part of the Gulf. Moreover, their results show a sedimentary layer beneath the Gulf of no more than 2.7 km.

An overall description of the 3D lithosphere and upper mantle P-wave structure has been presented in various tomographic studies (e.g. Spakman 1986; Christodoulou & Hatzfeld 1988; Spakman *et al.* 1988, 1993; Drakatos 1989; Drakatos *et al.* 1989; Ligdas *et al.* 1990; Drakatos & Drakopoulos 1991; Ligdas & Main 1991; Ligdas & Lees 1993; Papazachos *et al.* 1995; Tiberi *et al.* 2000). Papazachos & Nolet (1997) used travel-time data from local earthquakes in Greece and the surrounding areas and presented detailed results for the 3D P- and S-velocity structure of the Aegean lithosphere.

The published results on the lithospheric structure of the broader Aegean region based on measurements of the dispersion of surface waves are more limited. The early works of Papazachos *et al.* (1967) and Papazachos (1969) used group and phase velocities of Love and Rayleigh waves and studied the structure of the SE and Eastern Mediterranean region, respectively. Payo (1967, 1969) studied the structure of the Mediterranean Sea region using dispersion measurements of surface waves and identified a significant difference in the crust between the Eastern and Western Mediterranean, whereas Calcagnile & Panza (1980) and Calcagnile *et al.* (1982) focused on the regional study of the lithosphere–asthenosphere structure in the Mediterranean region. More recently, Kalogeras (1993) and Kalogeras & Burton (1996) used group velocity measurements of Rayleigh waves and produced 1D shear-wave velocity models down to 60–70 km along some seismic ray paths in the broader Aegean region. Marquering & Snieder (1996) used a waveform inversion method, in which the synthetic seismograms are calculated using surface-wave coupling, and studied the S-wave velocity structure beneath Europe, western Asia and the NE Atlantic to a depth of 670 km. They showed that in Europe, where the ray density is highest, small-scale structures are recovered, such as the presence of high velocities associated with the Hellenic subduction zone. Saunders *et al.* (1998) used teleseismic receiver functions to investigate the crustal structure at two locations in western Turkey using seismic data recorded on small arrays of temporary broadband seismological stations, and their results showed that western Turkey is characterized by a crust of *c*. 30 km thickness whereas a thicker crust of about 34 km is observed in eastern Turkey.

Yanovskaya *et al.* (1998) studied the shear-wave velocity structure under the Black Sea and surrounding regions using surface-wave group velocities. Recently, Martinez *et al.* (2000) studied the shear velocity structure of the lithosphere–asthenosphere system under the broader Mediterranean region using group velocities derived from the Rayleigh wave fundamental mode, and Pasyanos *et al.* (2001) investigated the broader southern Eurasia and Mediterranean Sea region using group velocities of both Rayleigh and Love waves. Karagianni *et al.* (2002) applied a surface-wave tomography method to group velocities of Rayleigh waves to connect group velocity variations with tectonic features of the crust and the upper mantle in the Aegean region. Raykova & Nikolova (2000, 2003) used the dispersion properties of Rayleigh and Love waves to study the anisotropy and constructed 1D models for the crust and uppermost mantle in southeastern Europe by the simultaneous inversion of both dispersion curves. Meier *et al.* (2004) used the two-station method to calculate the phase velocity curves of the fundamental Rayleigh mode and inverted them for 1D models of S-wave velocity. They estimated an average depth of the Moho beneath Crete at *c*. 50 km depth and above this discontinuity they found very low S-wave velocities of about 3.5 km s^{-1}. More recently, Karagianni *et al.* (2005), using the group velocities of the fundamental mode of Rayleigh waves, derived a 3D tomographic image of the shear-wave velocity structure of the crust–uppermost mantle in the Aegean region and estimated a new 3D image of the crustal thickness at this area. Surface-wave tomography on teleseismic events has been used by Bourova *et al.* (2005) to provide a 3D image of the lithosphere beneath the Aegean Sea. Their resolution analysis, which varied from 200 to 800 km, shows that only large-scale lateral anomalies greater than 200 km can be revealed from their dataset.

In general, the previous studies in the broader Aegean region show the existence of strong variations of the crustal structure. A thin crust of about 20–30 km has been proposed for the back-arc area, whereas a significant crustal

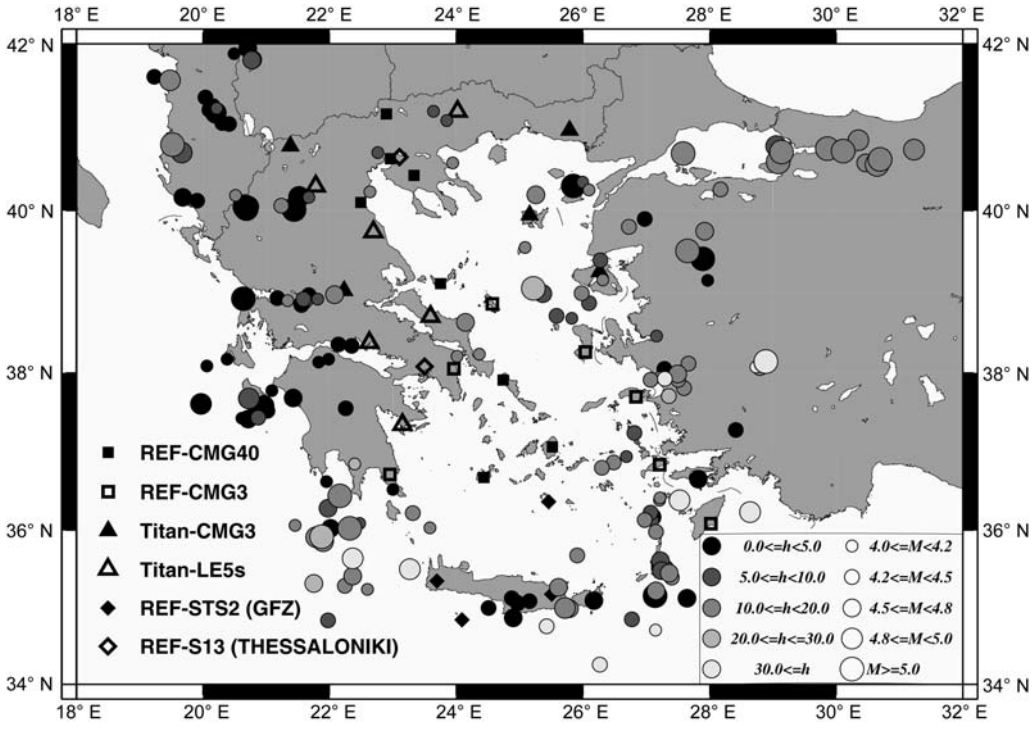

Fig. 2. Map of the epicentres of the events that were used in the present study and the locations of the portable stations. The earthquake depth and magnitude are shown by the grey shading and variable radius of the circles, respectively.

thickness (40–47 km) has been identified along the Hellenides mountain range. The crust has a normal thickness (28–37 km) in the eastern part of the Greek mainland, in the northern and central Aegean, in western Turkey and in Crete.

Unfortunately, 3D S-wave velocities for the Aegean region are not well known because of the limited number of body-wave tomographic studies on the S-velocity structure. The main purpose of this paper is to obtain a detailed 3D tomographic image of S-wave velocity for the uppermost *c*. 50 km in the Aegean region by combining Rayleigh and Love wave group velocities along different ray paths. These velocities were used to construct group velocity tomographic maps for different periods, ranging from 6 to 32 s, and jointly invert them to determine the 3D S-wave velocity structure of the study area.

Data

In the present study group velocity maps have been used as the main dataset for the S-velocity model determination. These maps represent the variation of the local group velocities of the fundamental mode of Rayleigh and Love waves for each type of wave at different periods and have been obtained by a tomographic inversion of single-path dispersion curves. These curves were computed for different single ray paths crossing the Aegean region, using the method of frequency time analysis (FTAN) of Levshin *et al.* (1972, 1989, 1992). We have considered 185 regional earthquakes within the area defined by 34–42° N and 19–31° E, which were recorded by 35 broadband stations of a temporary network that has been installed in the broader Aegean region. The locations of the events, as well as of the portable stations are shown in Figure 2, and a detailed description of these data has been given elsewhere (e.g. Hatzfeld *et al.* 2001).

Around 600 observed Love wave group velocity curves have been determined in this work, and we have also incorporated previous results for around 700 Rayleigh wave curves of the study area (Karagianni *et al.* 2002). The observed dispersion curves of Rayleigh waves have been calculated using the vertical component, Z, of the waveforms. The two horizontal components (east–west and north–south) of each record were rotated to a radial R (along the great-circle path) and transverse T component (perpendicular to the great-circle path) and the transverse component was used to estimate the

dispersion curves of Love waves. An example of the vertical and transverse components of a seismic record for an earthquake located in the Ionian Islands and used in the present study is shown in Figure 3. The ability of the analyst to identify the direct fundamental mode arrival and to distinguish it from higher modes, other reflections or coda waves is critical for the frequency bandwidth for which a dispersion curve can be estimated. A detailed description of the FTAN method has been presented in an earlier study (Karagianni *et al.* 2002). As the mean path length is of the order of 400 km, the Rayleigh and Love waves have been well recorded in the period range from 5 s to 30–35 s. This is also shown in Figure 4, where two FTAN maps for the components of Figure 3 for both Rayleigh and Love waves are shown. The FTAN method was applied for different (crossing) ray paths, and the coverage of the study area for a period of 10 s for both Rayleigh and Love waves is shown in Figure 5. As can be seen, the azimuthal distribution of the paths for both Rayleigh and Love waves is uniform and the coverage is satisfactory, especially in the central Aegean, where a large number of portable stations were located. Poorer density of seismic ray paths is observed in western Greece, NNE Greece and SW Crete because of the lack of earthquakes and recording stations.

Methods of analysis of surface waves

Tomography method

The group velocity curves of Rayleigh and Love waves for different ray paths estimated from the FTAN program have been used to construct the group velocity tomographic maps for different periods. For this purpose we have used a generalized 2D linear inversion method of Ditmar & Yanovskaya (1987) and Yanovskaya & Ditmar (1990), which is a generalization to two dimensions of the classical 1D method of Backus & Gilbert (1968) and is appropriate for regional studies as a solution is constructed on a plane surface obtained after transformation from spherical coordinates (Yanovskaya 1982; Jobert & Jobert 1983; Yanovskaya *et al.* 2000). The result of the surface-wave tomography is the estimation of local values of group velocity for each wave type at different grid points over the study area, which is used to obtain group velocity maps for different periods.

In tomography, the knowledge of the resolution is important to estimate the minimum resolvable features for a given sample and to determine those features that may be a numerical artefact. Yanovskaya (1997) and Yanovskaya *et al.* (1998) proposed the use of two parameters as resolution measures.

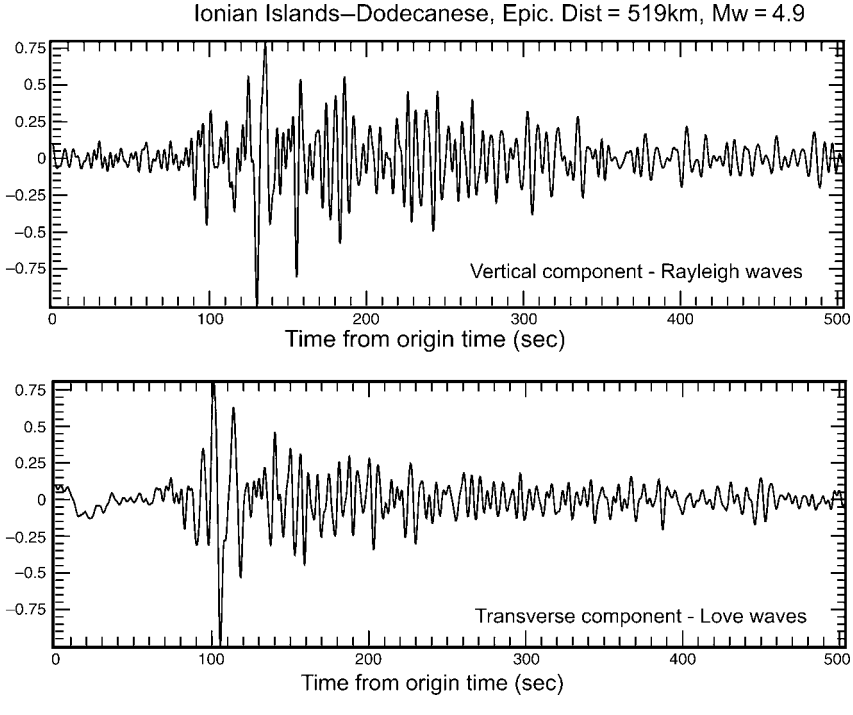

Fig. 3. Vertical and transverse components of a seismic record for a selected earthquake located in the Ionian Islands, used in this study to calculate the dispersion curves of Rayleigh and Love waves, respectively.

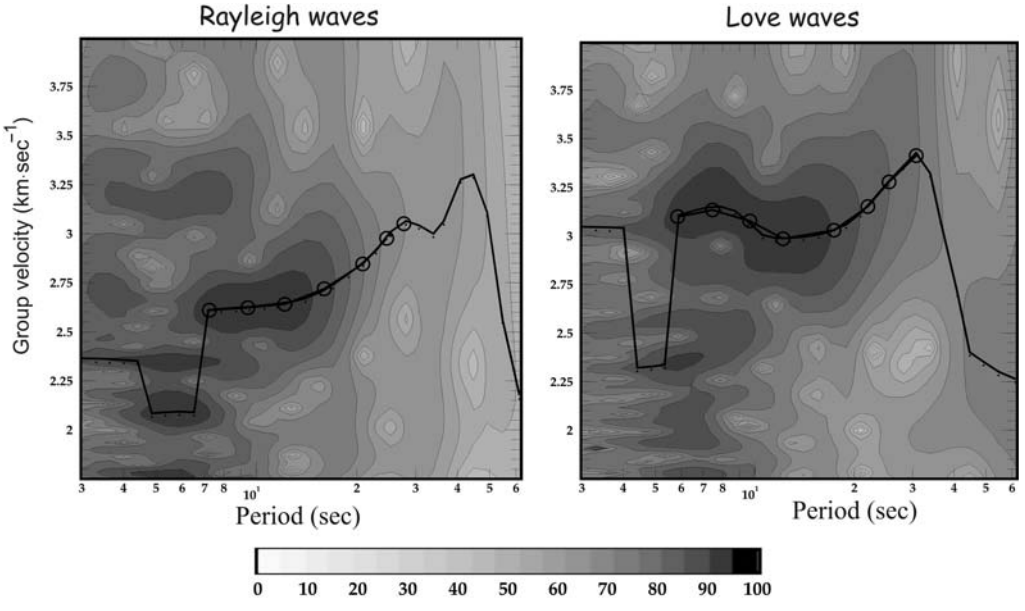

Fig. 4. Calculated FTAN maps of Rayleigh and Love waves, as estimated from the components of Figure 3. The continuous line indicates the dispersion curve that was identified by the analyst.

The first resolution parameter is the mean size of the averaging area, L, given by

$$L = [s_{\min}(x, y) + s_{\max}(x, y)]/2 \qquad (1)$$

where $s_{\min}(x, y)$ and $s_{\max}(x, y)$ are respectively the smallest and largest axes of an ellipse, which the averaging area can be approximated to, centred at each examined point (x, y). As the resolution is closely correlated to the density of the crossing ray paths in each cell, it is clear that small values of the mean size of the averaging area (corresponding to high resolution) should appear in the areas that are crossed by a large number of ray paths and vice versa.

The second parameter is the stretching of the averaging area, which provides information on the azimuthal distribution of the ray paths and is given by the ratio

$$2[s_{\max}(x, y) - s_{\min}(x, y)]/[s_{\max}(x, y) + s_{\min}(x, y)]. \qquad (2)$$

Small values of the stretching parameter imply that the paths are more or less uniformly distributed along all directions, hence the resolution at each point can be represented by the mean size of the averaging area. In contrast, large values of this parameter (usually >1) mean that the paths have a preferred orientation and that the resolution along this direction is likely to be small (Yanovskaya 1997).

Inversion method

In this study we employed the Hedgehog nonlinear inversion method for the determination of the S-wave velocity structure using the dispersion curves of surface waves (Keilis-Borok & Yanovskaya 1967; Valyus 1968; Knopoff 1972; Biswas & Knopoff 1974; Calcagnile & Panza 1980; Panza 1981). The Earth model is represented by a set of parameters (P- and S-wave velocities, and densities in a layered Earth), which may be varied or held fixed in the inversion and can be either independent or dependent, on the basis of *a priori* knowledge. For the independent parameters acceptable models are sought, whereas the dependent parameters maintain a fixed relationship with the independent ones. The ratio between S- and P-wave velocities, as well as the P-wave velocity and the density, are kept fixed in the inversion process because the phase velocity of the fundamental mode of Love waves is mainly sensitive to the shear-wave velocity (e.g. Urban *et al.* 1993). For that reason, only the S-wave velocities and the layer thicknesses were chosen as independent parameters.

For the inversion each parameter was specified to vary within a particular range, with upper and lower limits. The bounds within which we have allowed the independent parameters to vary are large enough that a large number of models are tested but at the same time these limits have been chosen so that the resulting velocities do

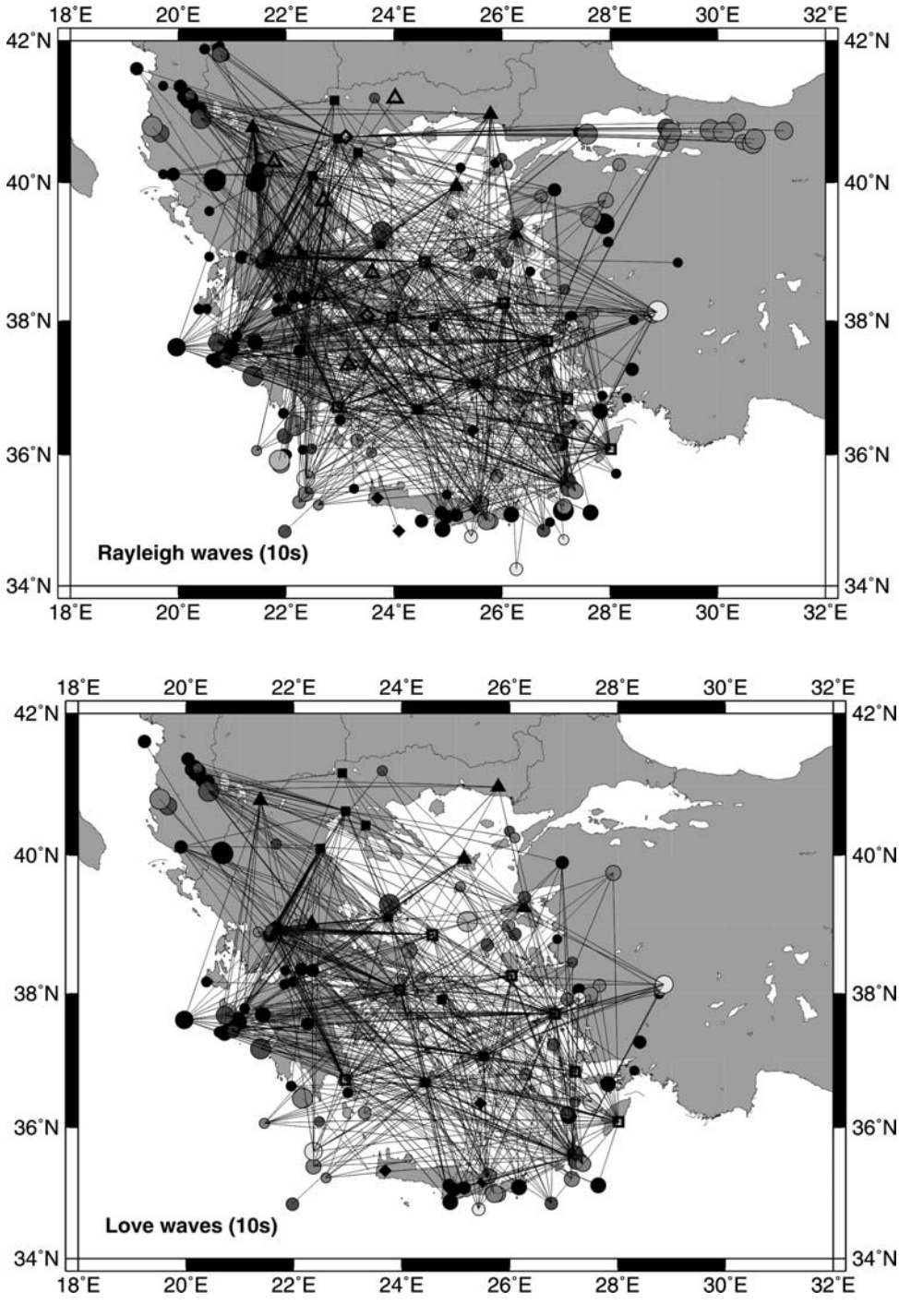

Fig. 5. Coverage of the ray paths used in this study for a period of 10 s for both Rayleigh and Love waves. Symbols as in Figure 2.

not reach unrealistic values. In addition, the steps used for the parameter variation should be properly chosen because large steps may exclude examining some models, whereas steps that are too small could result in an unnecessarily large number of tested models. For that reason the steps for the variation of the velocity parameters have been estimated according to the resolving power of the information contained in the available data (Panza 1981).

After perturbing the chosen set of model parameters within the pre-assigned parameters space, a set of theoretical values of group velocities (of Rayleigh wave first in the present study) are computed using the Knopoff method (Knopoff 1964; Schwab & Knopoff 1972; Schwab *et al.* 1984). Starting from the largest period, the theoretical group velocity is computed and compared with the observed value for the specific period. If the difference lies within the observational errors depending upon the quality of the measurements (single point error) the inversion proceeds to test the next shorter period, and so on. If the test is successful at all periods of the dispersion curve, the r.m.s. difference (root mean square deviation) between theoretical and observed values of group velocity of Rayleigh waves is computed and compared with a value defined *a priori* on the basis of the quality of the data. After tests, we set this value to 60% of the mean value of the single point experimental error of group velocity values, to avoid artificial large jumps of the theoretical dispersion curves or solutions with a systematic bias with respect to the experimental curve. On the other hand, if the test fails at any period, the model is rejected and a new model in the neighbourhood of the previous one is tested.

Models that pass both above-mentioned criteria were accepted for the case of Rayleigh waves and were then tested with the observed dispersion curves of Love waves using the same procedure and quality criteria. In general, Love wave data exhibit larger errors than Rayleigh waves, as Love waves are recorded in the horizontal component, which is more noisy than the vertical one, and hence it is more difficult for the analyst to accurately identify the Love wave dispersion curve. For grid points with a good path coverage the typical single point error for the case of Rayleigh waves is usually less than $0.06\,\mathrm{km\,s^{-1}}$, and is larger for the case of Love waves. These errors become generally larger for both wave types at the borders of the study area, where the number of crossing rays was limited. The same process was repeated until the neighbourhood around each satisfactory combination of the search parameters was explored.

Tomographic images of group velocity variations

As the group velocity variations of Rayleigh waves have been discussed in detail in previous studies (Karagianni *et al.* 2002, 2005), we present here only the group velocity maps of Love waves, shown in Figure 6 for six period values. In this figure we present results only for areas where the mean size of the averaging area is less than 200 km. Moreover, we have also plotted on each map the 100 km contour for the mean size of the averaging length for comparison. The variations are shown as percentages, relative to the corresponding mean velocities, which are also listed for each period. In general, the group velocity maps show significant lateral velocity heterogeneity, with variations up to 30% in the study area. At shorter periods (7–14 s) Love wave maps show significant low-velocity anomalies in western Greece under the Hellenides mountain range and in northern Greece in the Axios basin, as a result of the thick sedimentary formations in these areas, also identified in the tomographic maps of Rayleigh waves (Karagianni *et al.* 2002). Whereas for this period range a clear low-velocity layer in the southern Aegean Sea was dominant for the case of Rayleigh waves, the corresponding maps of Love waves for this period range do not exhibit a similar pattern. A possible explanation for this difference is that the structure at a certain depth affects Love wave dispersion curves at larger periods than Rayleigh waves. As the period increases an increase of Love group velocities is observed all over the Aegean Sea, as a result of the thin crust of the region. In contrast, low-velocity anomalies are clearly observed in western Greece, suggesting that the crust there is thick. At a period of 28 s the group velocity maps of Love waves show high velocities in the south and central Aegean Sea, whereas for larger periods (32 s) a low-velocity anomaly is found between Crete and the volcanic arc. A similar velocity anomaly in this area was depicted in the group velocity maps of Rayleigh waves for a period of 28 s.

The resolution parameters associated with the local group velocities of Love waves are shown for two periods (7 and 32 s) in Figure 7, and it can be seen that their values are more or less the same as those for Rayleigh waves (Karagianni *et al.* 2002). The mean size of the averaging area (quantifying the resolution of the local group velocity distribution) is of the order of 40–90 km in the central part of the Aegean and becomes larger (*c.* 150–200 km) only at the borders of the maps, where the path coverage is limited. The values of the stretching parameter of the averaging area generally indicate that the azimuthal distribution of the

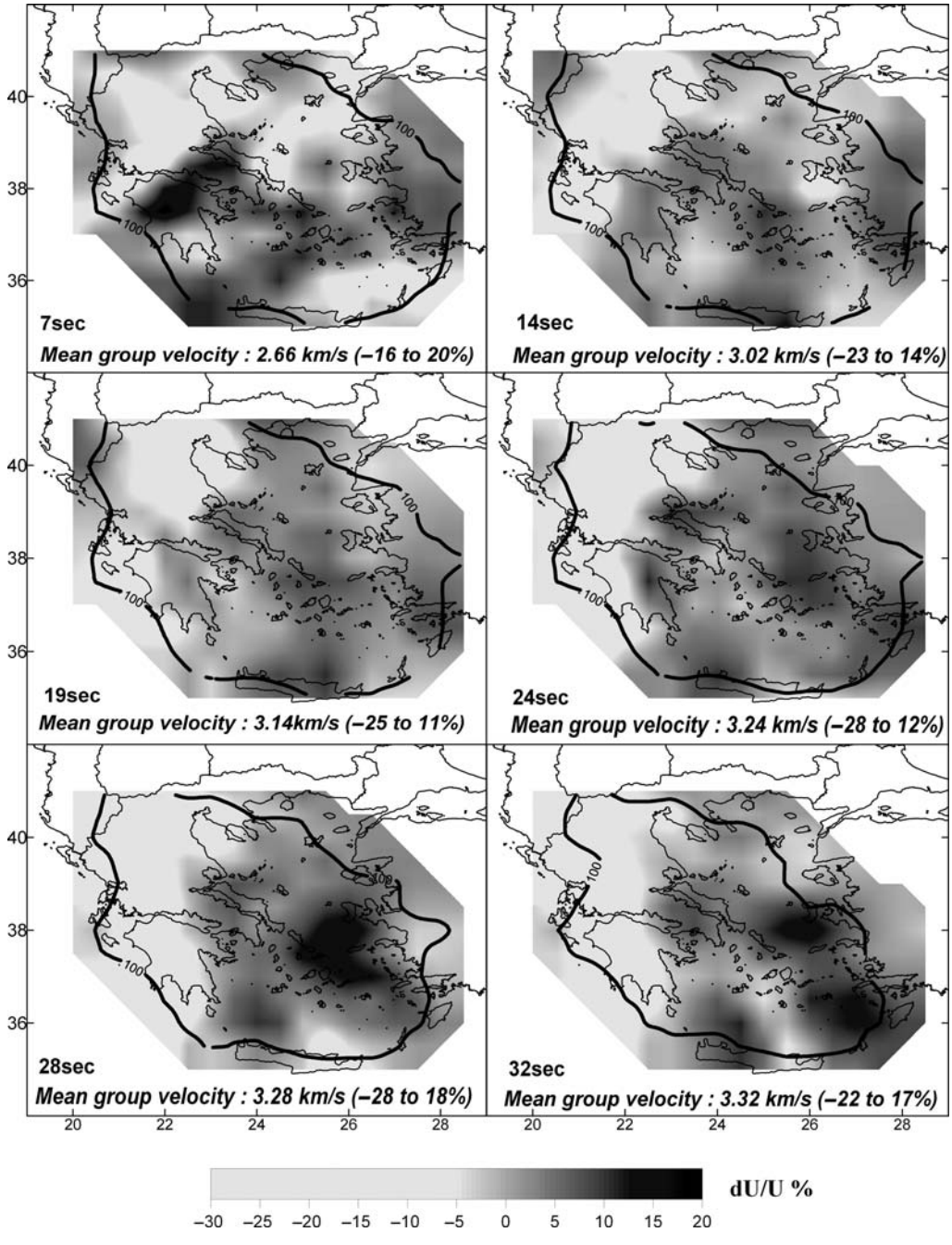

Fig. 6. Estimated Love wave group velocity maps at selected periods. Maps represent lateral variations (in %) of group velocity, relative to the average group velocity across each map.

paths is uniform, as this parameter has values smaller than one for most parts of the study area, and only at the borders of the area where the path coverage is poorer do we obtain values of one or larger. The standard errors of the local group velocities of Love waves are larger than those of Rayleigh waves and range between 0.07 and 0.12 km s^{-1} for all the examined periods.

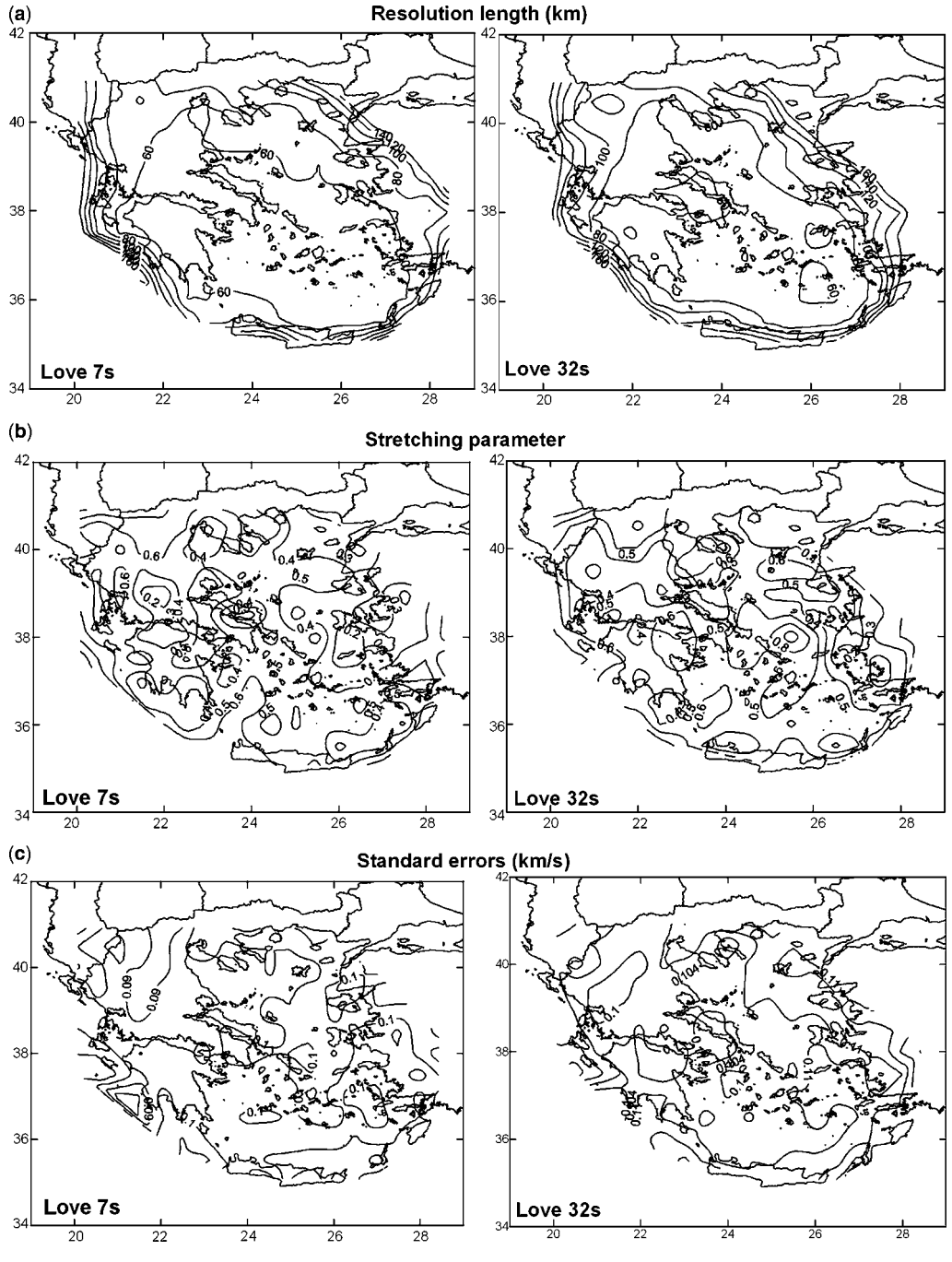

Fig. 7. Resolution information for the smaller (7 s) and the larger period (32 s) used in the present study: (**a**) resolution length (in km); (**b**) distribution of the elongation of the averaging area; (**c**) standard error (in km s^{-1}) associated with the estimated group velocity maps.

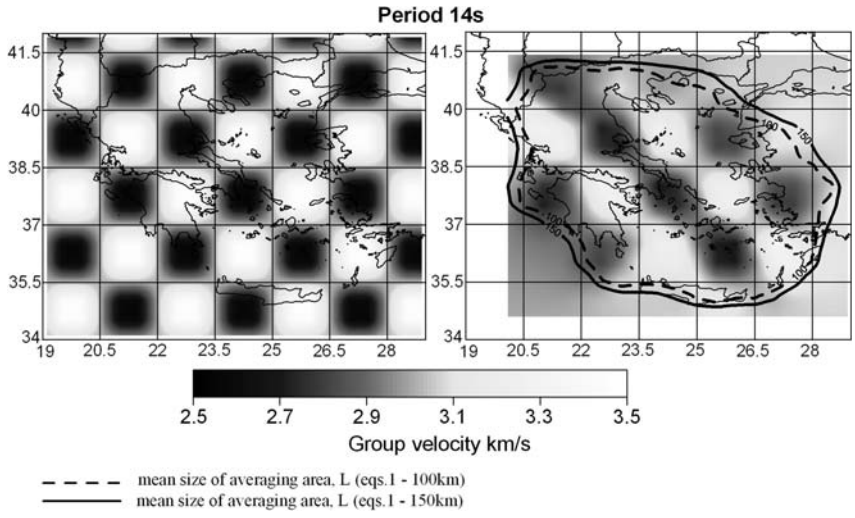

Fig. 8. Chequerboard test for 14 s Love wave using a cell of $1.5^\circ \times 1.5^\circ$ (typical anomaly size *c.* 150km), using a sinusoidal velocity perturbation with a peak amplitude of $\pm 20\%$.

To further explore the resolving information of the tomographic results of the joint inversion of Rayleigh and Love waves we have performed additional resolution tests. For this reason, we divided the study area into cells and applied a sinusoidal velocity perturbation with respect to the average group velocity for each examined period. Using this model, travel times along paths linking source and recording stations were calculated, adopting the same ray coverage configuration as in Figure 5b. A solution for these velocity perturbations was obtained using the same regularization parameters as for the real data in the tomographic inversion. The chequerboard test was performed for different cell sizes, as well as for different values of the velocity perturbation. In Figure 8 we show the results of the chequerboard test for a period of 14 s using perturbation anomalies with a peak amplitude of 20% and a length of *c*. 150 km. Moreover, the contour lines of 100 and 150 km for the mean size of the averaging area for the real data are also superimposed. We observe that the well-resolved area (according to the chequerboard tests with anomalies *c*. 150 km) is in very good agreement with the corresponding contour of 150 km for the mean size of the averaging area, which verifies the reliability of the resolution estimates shown in Figure 7.

Inversion results

From the estimated group velocity maps a local group velocity of Rayleigh (Karagianni *et al.* 2002) and Love waves has been constructed for different grid points over the Aegean region. Finally, a mean local dispersion curve with its standard error for each type of wave was assigned to each $0.5^\circ \times 0.5^\circ$ grid cell using the dispersion curves that corresponded to the four corners of each cell. Because the patterns of paths for Rayleigh and Love waves are slightly different for different periods, we may expect a difference between the velocity sections obtained from Rayleigh and Love waves separately. Moreover, it is well known that the velocities determined from Rayleigh and Love waves can differ because of the possible anisotropic properties of the crust and upper mantle. To reduce the errors arising from differences of the pattern paths, we have jointly inverted the Rayleigh and Love wave dispersion curves. Sixty mean local dispersion curves of Rayleigh and Love waves were inverted, producing vertical 1D shear-wave velocity models for different examined points. After the inversion, a simple bilinear interpolation scheme was adopted and a 3D image of the S-wave structure was derived for depths ranging from 5 to 45 km.

Despite the fact that with the adopted nonlinear inversion scheme the starting model does not significantly affect the final results, the starting model of S-wave velocities for the inversion has been taken from the work of Papazachos & Nolet (1997) and Martinez *et al.* (2000), who gave detailed information on the 3D S-wave velocity structure of the Aegean lithosphere. Furthermore, information on the shear velocity structure of the study area from Karagianni *et al.* (2005), based on the inversion only of Rayleigh waves, has been also considered. For the cases where the inversion

was performed at grid points located in the sea, the starting 1D model was overlain by a water layer of variable thickness (0.2–2.5 km), according to the bathymetric map for the broader Aegean region. This was important only for Rayleigh waves, as the water layer does not affect the propagation of Love waves. Our data are not adequate to resolve the elastic properties of the very shallow layers, or those of the deep mantle (greater than 45–50 km). For this reason these properties were kept fixed, using existing results from the previously mentioned literature. In particular, the elastic properties (the S-wave velocities and the layer thickness for the upper 3–5 km) have been fixed on the basis of information coming mainly from seismic soundings by the Greek Public Petroleum Company (N. Roussos, pers. comm.) and from other existing geophysical investigations (e.g. Makris 1976, 1977; Martin 1987; Roussos 1994). The P-wave velocities have been defined on the basis of S-wave velocity values, using the V_P/V_S values given by Papazachos & Nolet (1997). The density values that were used in the present study have been calculated from the values of P-wave velocities using the relationship of Barton (1986) for crustal and upper mantle material.

For each examined grid point, 8–10 parameters have been allowed to vary in the inversion scheme; namely, the S-wave velocities in 4–5 layers reaching a depth of about 40–45 km, as well as their related thicknesses. In the inversion process for each examined point we considered the depth of 45–50 km as a maximum depth at which the independent parameters were allowed to vary. This is based upon the variation of the group velocity sensitivity kernels on the shear-wave velocity v. depth (Panza 1981; Urban *et al.* 1993), as has already shown in detail in the previous work of Karagianni *et al.* (2002).

In Figure 9 we present the inversion results for a common depth range (26–30 km) after the independent inversion of Rayleigh and Love waves. In general, these images show high S-wave velocities (4.0–4.3 km s^{-1}) in the Aegean Sea (typical upper mantle velocities), whereas crustal S-wave velocities (*c.* 3.5 km s^{-1}) are observed in western Greece. Love wave inversion exhibits slightly higher S-wave velocities compared with the Rayleigh wave data, especially in the Aegean Sea region (lower crust, uppermost mantle). However, the high S-wave velocities resulting from Rayleigh wave inversion extend over a larger area in the Aegean Sea compared with the S-wave velocities of Love wave inversion. The critical point is whether this bias reflects specific model properties (e.g. anisotropy) or whether a subset of the models derived from the Hedgehog inversion could explain both Rayleigh and Love wave group velocity data. To examine this issue, we performed a joint inversion of Rayleigh and Love wave data to search for models that satisfy both experimental dispersion curves of Raleigh and Love waves. As an example, we present the results for an examined grid point in the central Aegean Sea in Figure 10, where the experimental and the theoretical dispersion curves of both waves are depicted. It can be observed that Love wave group velocities are larger than the velocities of Rayleigh waves for all periods, and also exhibit larger errors. However, the experimental–theoretical dispersion curve fit for both types of waves is fairly good and does not appear to follow a systematic pattern (e.g. systematic underestimation of Love group velocities). These results are representative of almost all the examined grid points, with larger discrepancies observed only for a few grid points at the margins of the examined area.

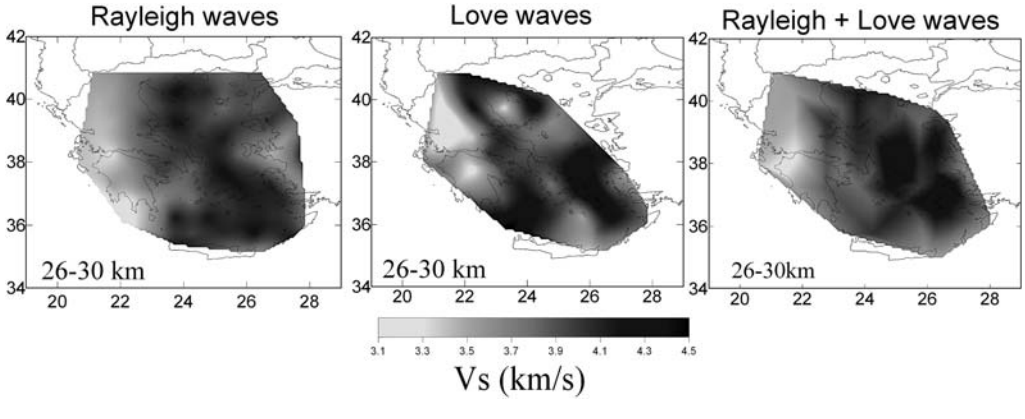

Fig. 9. Horizontal cross-section of the shear-wave velocity model for the depth range 26–30 km in the Aegean region, as derived from the independent inversion of Rayleigh and Love waves, as well as the joint inversion of the both waves.

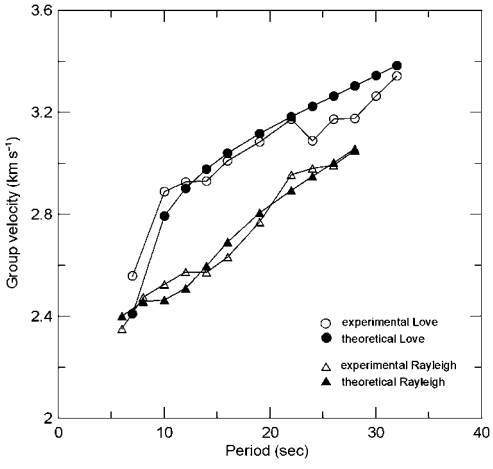

Fig. 10. Experimental and theoretical dispersion curves for a selected grid point.

On the basis of these results we suggest that the joint inversion of both Rayleigh and Love waves can give more reliable results by selecting a small number of velocity models that are compatible with both datasets. This is confirmed in Figure 11, where for a random grid point in the study area we show the inversion results using only Rayleigh wave data, Love wave data and jointly Rayleigh and Love wave data. The solutions that are estimated from the joint inversion of Rayleigh and Love waves do not reflect the average of the individual solutions but correspond to models that satisfy both Rayleigh and Love wave group dispersion data. This is why the number of accepted solutions in the simultaneous inversion of Rayleigh and Love wave data has been significantly decreased compared with the solutions of the independent inversion of Rayleigh and Love wave data. Nevertheless, most of the solutions of the above three inversion schemes show similar structural

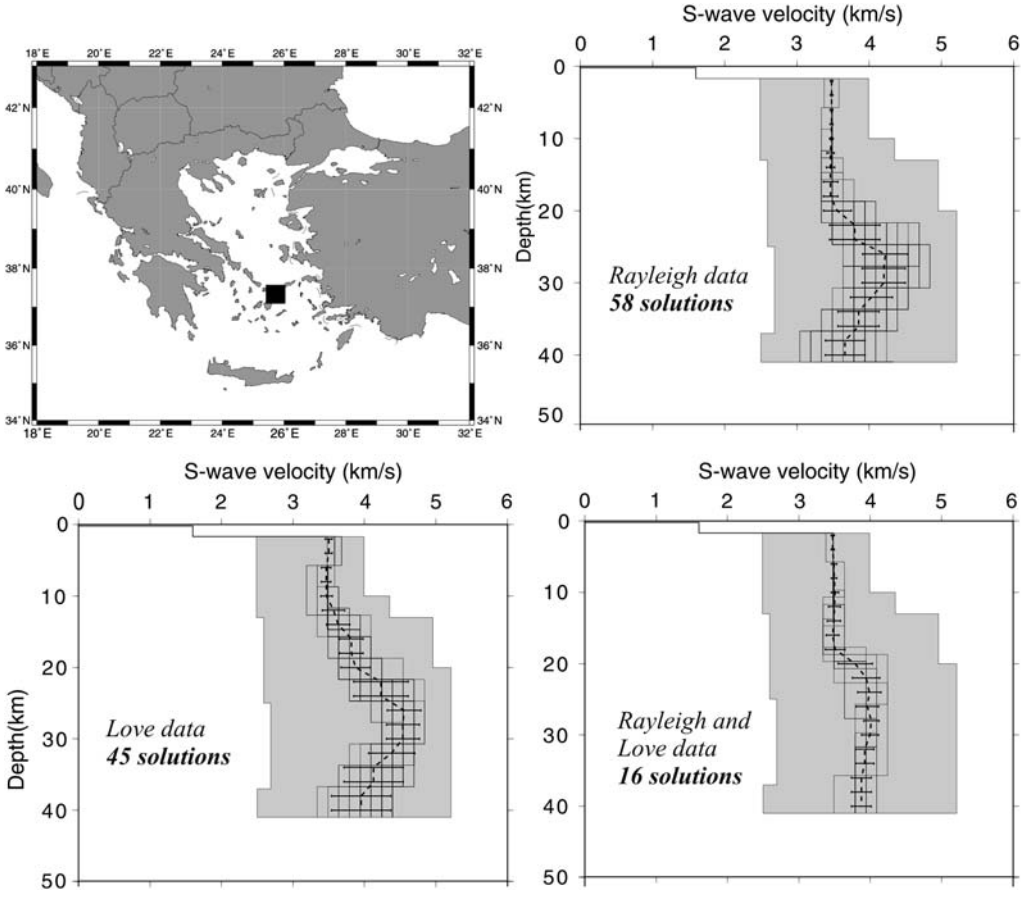

Fig. 11. Final S-wave models for a grid cell in the Aegean Sea after the independent inversion of Rayleigh and of Love waves, and the joint inversion of both types of surface waves.

features. These are the Moho discontinuity, which is shown at a depth of about 20–22 km, as well as a decrease in velocity just below the Moho, which is interestingly more evident when Rayleigh and Love wave are inverting separately.

S-wave velocity variations

A 3D image of the Moho discontinuity for the study area was constructed using the local 1D vertical models of shear-wave velocity, as derived from the inversion process for each geographical point examined. Using all the solutions of the inversion the average S-wave velocity was estimated using a depth interval of 2 km to define the average S-velocity depth profile at each point. We have assumed that a shear-wave velocity of about 3.9–4.0 km s^{-1} is a reasonable approximation for the S-wave velocity at the bottom of the lower crust. The depth at which we observed a significant jump in the S-wave velocity that 'crossed' this limit of 3.9–4.0 km s^{-1} (e.g. from 3.8 to 4.3 km s^{-1}) was assumed to be the Moho discontinuity. However, for some solutions a smooth transition rather than a steep jump was observed in the S-wave velocity from the lower crust to the upper mantle, in which cases a Moho depth was not assigned. On the other hand, because for each grid point several solutions existed, this resulted in not assigning a Moho depth only for a small number of solutions for each grid point (typically *c*. 20%).

Significant lateral change in the crustal thickness can be observed in Figure 12a, as is expected from the tectonic complexity of the Aegean region. Western Greece, with the presence of the Hellenides mountains, is dominated by a thick crust of the order of 40–45 km. As we move to the east the crust becomes thinner, and most of continental Greece is characterized by a normal thickness of crust of about 34–38 km. Some parts of eastern continental Greece (e.g. the island of Evia) have a thinner crust of about 28 km. The most interesting feature is that the whole Aegean Sea is characterized by a thin crust, typically less than 28–30 km. In some parts in the southern and central Aegean Sea a significantly thinner crust of about 20–22 km is observed, in agreement with the north–south extensional field (Fig. 1), as well as with the rise of hot mantle material owing to the subduction of the eastern Mediterranean plate under the Aegean microplate. The north Aegean Sea is also characterized by a thin crust, and a crustal thickness of about 25 km is observed near the North Sporades islands. Only in some parts of the north Aegean Sea (between the islands of Lemnos and Lesvos) does the crust show a thickness of about 32–34 km. Results are not shown for the borders of the Aegean region (NE Greece and Crete) because the inversion process did not give models that satisfied both experimental Rayleigh and Love wave data, resulting either from the larger errors of the experimental curves at the borders of the study area or from the presence of anisotropy. However, the above-mentioned results are in agreement with those in previous investigations (e.g. Makris 1976; Brooks & Kiriakidis 1986; Chailas *et al.* 1993; Papazachos 1994, 1998; Karagianni *et al.* 2005).

Using all the estimates for the Moho depth at each grid point where the joint inversion of Rayleigh and Love waves has been performed (as described above), we have also estimated (Fig. 12b) the corresponding standard deviation of the Moho depths and used it as an error estimate of the Moho depth map of Figure 12a. It is observed that for the largest part of the study area the estimated error is less than 4 km, which is acceptable considering the wide range within which the Moho depth discontinuity varies (more than 25 km). The relatively small error of the Moho depth discontinuity confirms that most of the acceptable solutions of the inversion give similar values for the Moho depth, despite the large parameter space that the inversion was searching for solutions. Only at the borders of the study area does the error become larger than 4 km, as the data coverage is poor (group velocity along different ray paths), resulting in low resolution. Of course, the presented errors reflect only the data variability and cannot account for any additional errors in our estimation as a result of the limitations or the assumptions of the inversion approach.

Using the 1D S-wave models derived in this study we have constructed several horizontal velocity sections for different depths, shown in Figure 13. The shallow depth sections (6–16 km) are characterized by relatively low S-wave velocities for most of the study area. The direction of these low-velocity anomalies more or less follows the known Dinaric trend (NNW–SSE) in NW Greece and then changes to ENE–WSW in the central and southern Aegean Sea, becoming almost east–west in western Turkey. These depicted anomalies roughly coincide with the active fault zones in the Aegean region, which are the result of the NNW–SSE extension process in the broader Aegean region, as well as with the westward escape of the Anatolian plate (e.g. McKenzie 1972; Taymaz *et al.* 1991).

The S-wave velocity image changes as we move to greater depths (16–20 km), as velocities larger than 3.5 km s^{-1} (which are typical values of the lower crust) are found in the northern and southern Aegean Sea, whereas smaller velocities are observed for the remaining part of the study area.

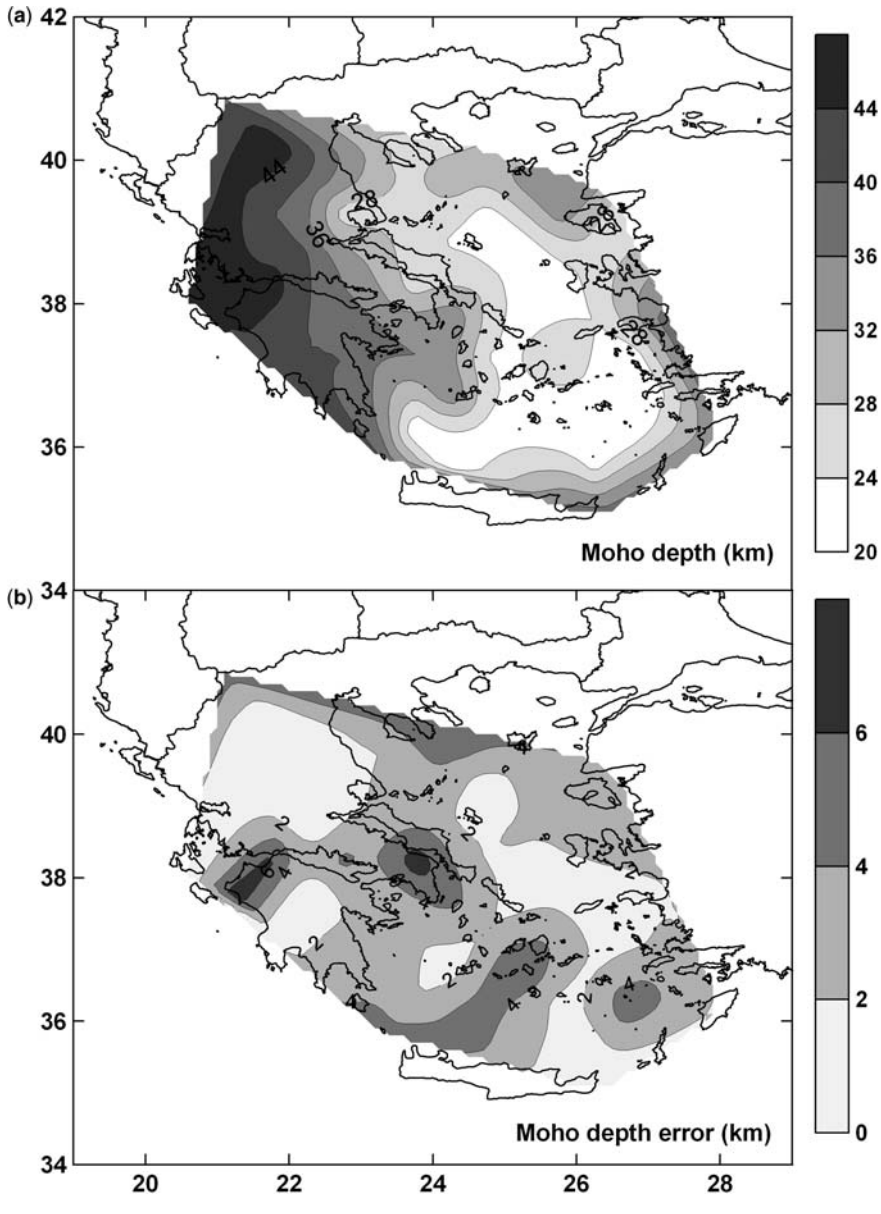

Fig. 12. (**a**) Moho depths (km) for the broader Aegean region estimated from the joint inversion of Rayleigh and Love waves. (**b**) Estimated error (in km) of the Moho discontinuity.

For the depth range of 20–26 km typical velocities of the lower crust (3.6–3.8 km s^{-1}) are observed in eastern continental Greece, whereas larger velocities of about 4.1–4.2 km s^{-1} are observed in SE Aegean Sea, indicating the presence of uppermost mantle. Similar S-wave upper mantle velocities have been found by Kalogeras (1993) along three paths that cross the south Aegean Sea (Karpathos–Athens, Rhodes–Athens and SW Turkey–Athens). Lower S-wave velocities are still present in western Greece, which probably correspond to middle–lower crustal levels.

To a depth of about 30 km S-wave upper mantle velocities (4.0–4.4 km s^{-1}) dominate throughout the Aegean Sea, whereas crustal S-wave velocities (*c.* 3.5 km s^{-1}) are still observed in western Greece, confirming the difference in crustal thickness between continental Greece and the Aegean

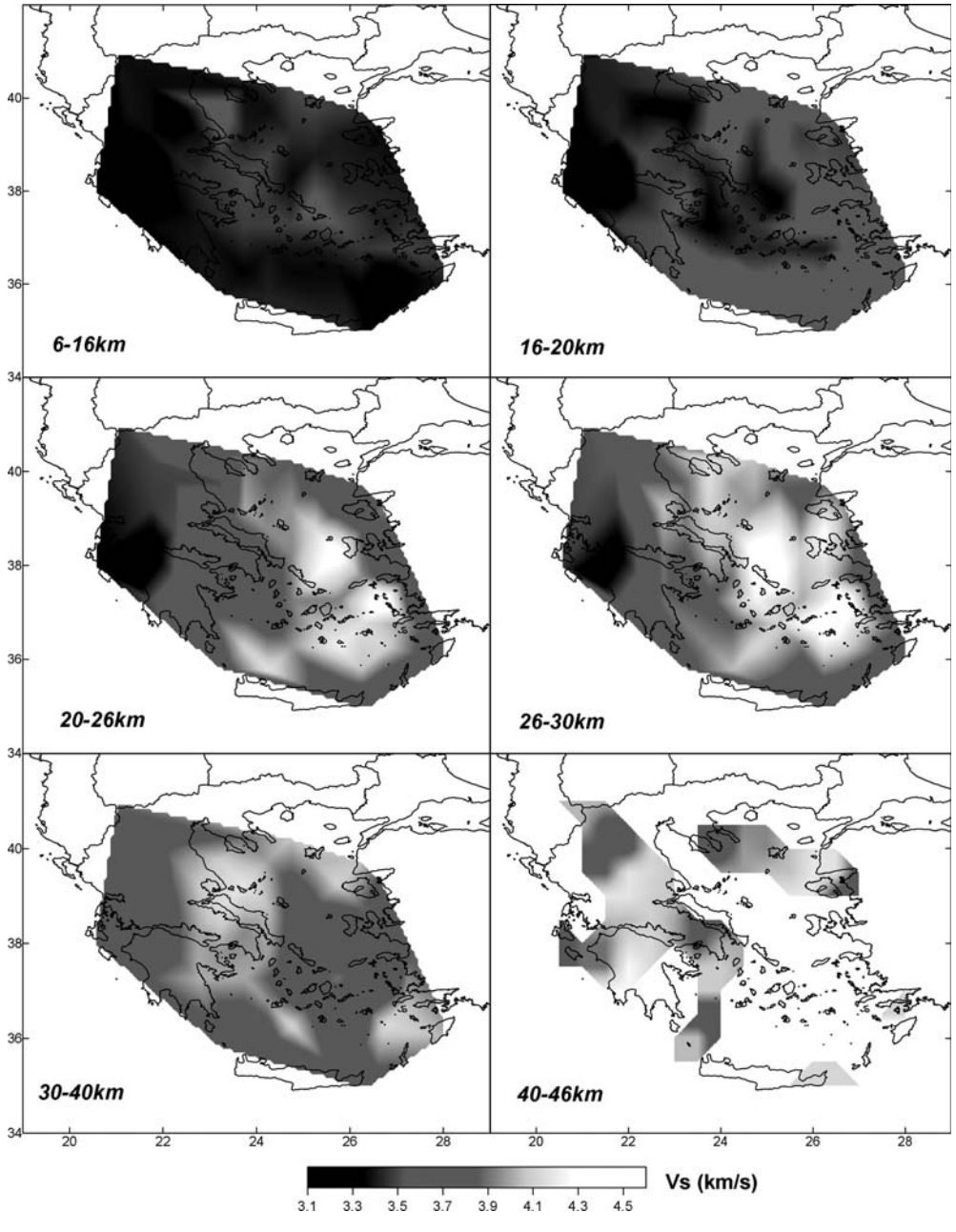

Fig. 13. Horizontal cross-sections of the final shear-wave velocity model for the Aegean region at different depth ranges.

Sea. The S-wave upper mantle values that have been observed in some parts of the study area are lower than typical upper mantle values throughout most of Europe. Similarly low S-wave upper mantle velocities have been found also for Turkey by Mindevalli and Mitchell (1989).

For depths ranging from 30 to 40 km the high upper mantle S-wave velocities in the southern and central Aegean Sea change to relatively low S-wave velocities (3.6–3.8 km s^{-1}). These low S-wave velocities are observed just below the Moho discontinuity and can be correlated with

the uplift of hot mantle materials and high surface heat flow (Hurtig *et al.* 1991). Moreover, low upper mantle velocities have been also found in body-wave tomographic studies (Spakman 1986; Spakman *et al.* 1993; Papazachos & Nolet 1997). A similar situation has been observed along the active (seismically and volcanically) side of the Tyrrhenian Sea and bordering land (Pontevivo & Panza 2002; Panza *et al.* 2004). Kalogeras & Burton (1996) detected similar low S-wave velocities at a depth of about 30 km along three paths (Karpathos–Athens, Rhodes–Athens and SW Turkey–Athens) that cross the southern Aegean Sea. Taymaz (1996) suggested that both P- and S-wave velocities in the crust and upper mantle of the Aegean are notably lower than those beneath the Hellenic Trench near Crete, which he partly attributed to high heat flow values in the Aegean back-arc in contrast to low heat flow values in the Sea of Crete. This is also in agreement with the work of Gok *et al.* (2000), who provided an attenuation study of regional shear waves (Sn and Lg) in the northern Aegean and Greek mainland area and showed that an inefficient Sn propagation along the volcanic arc is due to the low upper mantle velocities and high attenuation observed in this area. The very low S-wave velocity anomalies in the mantle wedge (*c*. 10%, locally up to *c*. 15%) obtained in the present study (V_S *c*. 3.7 km s^{-1}) in combination with the P-wave velocity anomalies from body-wave tomography (*c*. 5–6%, locally 7% with V_P *c*. 7.3–7.4-km s^{-1}) verify the presence (Karagianni *et al.* 2005) of an unusually high V_P/V_S ratio of 1.9–2.0 in the mantle wedge of the southern Aegean Arc. The combination of such low velocities with high V_P/V_S values corresponds to the presence of a high fraction (*c*. 15–20%) of partial melt in the mantle wedge for a typical mantle composition (e.g. Birch 1969), in agreement with existing results from petrogenetic analyses of volcanic rocks (Zelimer 1998), which also suggest a high degree of mantle melting (*c*. 15–20%) beneath the volcanic arc in the Aegean region.

Discussion and conclusions

The results of the joint inversion of Rayleigh and Love waves verify the existence of strong S-wave velocity lateral variations in the Aegean. Our inversion results suggest that there is no significant Rayleigh–Love discrepancy in the Aegean region and there are several isotropic models that can satisfy both Rayleigh and Love wave data. It should be noted that the amount of anisotropy in the upper mantle and lower crust is a matter of debate, especially in continental regions and in subduction zones (e.g. Montagner & Tanimoto 1991) Hatzfeld *et al.* (2001) studied the shear-wave anisotropy in the upper mantle beneath the Aegean region and found that little azimuthal anisotropy is observed along the Hellenic arc and in continental Greece, whereas significant anisotropy is observed in the north Aegean Sea. On the other hand, any observed Rayleigh–Love anisotropy should be mainly caused by radial anisotropy. Preliminary results show that radial anisotropy seems to be small or of very local character in the Aegean region at crustal–upper mantle levels, with typical values of *c*. 0–3% (e.g. Boschi *et al.* 2004; Endrun *et al.* 2006). Such small anomalies will have a weak influence on the joint Rayleigh–Love interpretation and in any case are much smaller than the corresponding velocity anomalies observed in the final 3D model (Fig. 13), which locally exceed 20%.

The most prominent feature confirmed in this work is the large crustal thickness contrast between western Greece (along the Hellenides mountain range) and the Aegean Sea (e.g. Fig. 13). In the southern Aegean Sea, as well as in parts of the central Aegean Sea, the crust has a thickness of about 20–22 km. This crustal thinning is associated with the extensional tectonics of the Aegean back-arc area and the rise of mantle material, as a result of the convergence between the Eurasian and African plates. Generally, the inner Aegean Sea shows a crustal thickness less than 28–30 km, whereas in western Greece a significant crustal thickness of about 40–46 km is observed along the Hellenides mountain range. A normal crust of thickness *c*. 30–34 km is observed in eastern continental Greece. The thin crust (20–22 km) between the volcanic arc and Crete has also been found in previous studies (e.g. Makris 1976; Bohnhoff *et al.* 2001) but the present study suggests for the whole Aegean Sea a thinner crust compared with previous works, in agreement with gravity data (Papazachos 1994; Tsokas & Hansen 1997; Tirel *et al.* 2004), which have indicated the presence of a thin crust (*c*. 25 km) throughout the Aegean Sea.

A low-velocity crustal layer at depths from 10 to 20 km along the Hellenic arc was observed by Papazachos (1994) and Papazachos *et al.* (1995), and was later confirmed by Papazachos & Nolet (1997) for the P-wave structure. This layer was correlated to the Hellenides mountain range and the Alpine orogenesis, in accordance with the ideas of weakening mid-crustal intrusions and the associated LVL, which was proposed by Mueller (1977). More recently, Karagianni *et al.* (2005) showed that this crustal low-velocity layer is also found in the S-wave structure, as obtained by the inversion of Rayleigh waves. The results of the joint inversion of Rayleigh and Love waves confirm the existence

of this low-velocity crustal layer along the outer Hellenic arc, as is also shown by the vertical cross-sections in Figure 14.

The results of the present study also confirm the presence of a strong low-velocity mantle wedge layer (MW LVZ) with S-wave velocities about of 3.7–3.8 km s^{-1} above the subducted slab in the southern Aegean Sea, as well as in a small part of the central Aegean Sea, whereas the remaining Aegean Sea and continental Greece exhibit more typical uppermost mantle velocities (*c*. 4.2–4.4 km s^{-1}). However, these values are still slightly lower than previously considered values mainly based on joint P- and S-wave travel-time inversions (e.g. Papazachos & Nolet 1997). The very low S-wave velocity anomaly that is found in the mantle wedge (associated with partial melting in the southern Aegean Sea) has also been observed in similar geotectonic environments, such as the Tonga, Alaska and Japan volcanic arcs (e.g. Zhao *et al.* 1995, 1997), with S-wave low-velocity anomalies locally exceeding 15%.

Our results seem to be in a very good agreement with independent information on the velocity structure (e.g. Papazachos 1993) as determined from several published results (deep seismic profiles, tomography, gravity inversion, etc.). In general, the surface-wave results tend to give a stronger crustal thinning for the central and southern Aegean Sea compared with previously published results. Moreover, there is relatively good agreement between our results and independent information, such as the work of Li *et al.* (2003), who used data from broadband seismographs on five islands in the southern Aegean Sea to construct receiver function images of the crust and upper mantle for the areas south of Crete and into the Aegean. They estimated a thin crust of about 25 km in the central Aegean Sea near Naxos, and a thicker crust of about 28 km for the SW coast of Asia Minor. For stations located in Crete, Li *et al.* showed that the depth of the Moho discontinuity varies from 32 to 39 km, which is in good agreement with our results. The only significant difference from our results is the Moho depth of 32 km estimated for Santorini, which is much thicker than our estimate of 22 km in the present study. However, more recent results (Endrun *et al.* 2005) show that the receiver functions in Santorini have been misinterpreted and a typical thickness of 23 km is determined from the receiver function data, in very good agreement with the thickness found in our study.

The results of this study were also compared against the independently determined 3D P-wave velocity model for the crust and uppermost mantle of the Aegean area (Papazachos & Nolet 1997). In Figure 14, the general features of the crustal thickness variation from P-waves (travel-time inversion of body waves) and S-waves (from surface-wave group velocity inversion) are also in good agreement for both examined cross-sections but again surface-wave results tend to show smaller crustal thickness values for the central part of the southern Aegean Sea. This is probably due to the poorer accuracy of catalogue phase-picks used in travel-time inversion, which often suffer from significant picking errors (up *c*. 0.5–1 s at regional distances, perhaps larger for S-waves), as well as from the lack of recording stations (and partly events) in the southern Aegean Sea region. Furthermore, the high upper-mantle velocities immediately below the Moho in the same area are clearly identified in both models. On the other hand, the P-wave tomography shows the low velocities associated with the mantle wedge above the subducted slab at depths of about 55–70 km (and locally at larger depths), whereas surface-wave models start to identify this low-velocity layer in the mantle at much greater depths (*c*. 35–40 km). Although the V_S model determined in the present study has no resolving power at greater depths because of the limited frequency range of the observed group velocity curves, it is expected that the effect of partial melt on S-wave velocities is much more pronounced compared with that on P-wave results. Therefore, this discrepancy should be attributed to the stronger melt signature in S-models, probably in combination with the crustal thickness overestimation for the thin crust areas from tomographic results owing to the damping and smoothing constraints usually applied when inverting travel-time data for large-scale models.

It should be pointed out that the amplitude of S-wave velocity anomalies from surface-wave inversion are significantly larger (up to more than 200% higher) when considering the S-wave structure from travel times (Papazachos & Nolet 1997). This effect is especially prominent for the southern Aegean mantle low-velocity layer, corresponding to the mantle wedge above the southern Aegean subduction zone, where very low uppermantle S-velocities are detected from surface-wave inversion, in agreement with independent information (Gok *et al.* 2000). These results suggest a possible bias not only of the tomographic approach in travel-time inversions but also of the original travel-time data, as large S-residuals are often rejected during the preliminary relocation procedures followed by most seismological networks. Moreover, additional factors such as anisotropy may need to be taken into account for such discrepancies, as well as for local Rayleigh–Love differences. However, the results obtained in the present study suggest that the V_S model obtained here is generally in good agreement with existing 3D

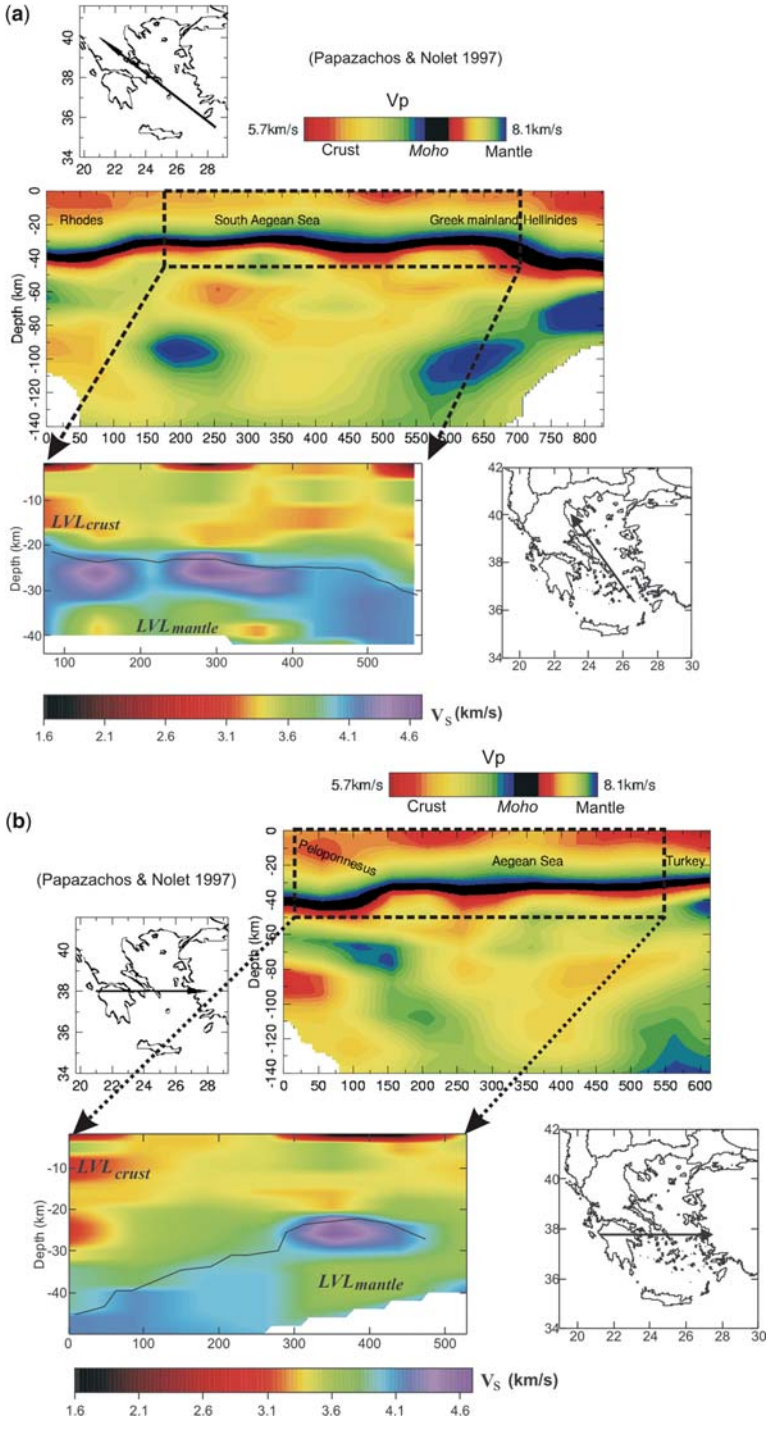

Fig. 14. (**a**) Comparison of the V_P model of Papazachos & Nolet (1997) with the V_S results obtained in the present study for a SE–NW cross-section in the study area. The similar crustal thickness variation in the two models and the high sub-Moho velocities in the southern Aegean Sea should be noted. However, the mantle LVL is detected at shallower depths in the V_S models than in the V_P models. (**b**) Same for a typical east–west cross-section.

P- and S-models (at least regarding its principal features and characteristics) and provides additional information on the true amplitude of S-wave anomalies that can be identified. Furthermore, this observation suggests that a joint inversion of travel-time and surface-wave data may be able to provide a single $V_P - V_S$ model that can simultaneously interpret both datasets by reducing the non-uniqueness of their inversion.

The data collection for this work was financed by the EC Environment and Climate project (contract ENV4-CT96-0277). We thank D. Hatzfeld and a large number of people for their effort to make the field experiments successful. We are grateful to A. Levshin for providing the FTAN code, and to T. Yanovskaya and P. Ditmar from the University of St. Petersburg, Russia, for providing the tomographic inversion program. We would like to thank the GeoForschungsZentrums, Potsdam, Germany, for providing the records from their network in the southern Aegean Sea. We would also like to thank Ş. Barış, an anonymous reviewer and T. Taymaz for their constructive comments and suggestions, which helped to improve this work. This work was partly financed by the project Pythagoras-Environment founded by EPEAEK (21945) and PEP of Crete (81106).

References

ANDERSON, H. & JACKSON, J. 1987. Active tectonics of the Adriatic Region. *Geophysical Journal of the Royal Astronomical Society*, **91**, 937–983.

BACKUS, G. & GILBERT, F. 1968. The resolving power of gross Earth data. *Geophysical Journal of the Royal Astronomical Society*, **16**, 169–205.

BARTON, P. J. 1986. The relationship between seismic velocity and density in the continental crust—a useful constraint? *Geophysical Journal of the Royal Astronomical Society*, **87**, 195–208.

BIRCH, F. 1969. Density and composition of the upper mantle: first approximation as an olivine layer: *In*: HART, P. J. (ed.) *The Earth's Crust and Upper Mantle Structure, Dynamic Processes, and their relation to Deep-Seated Geological Phenomena.* Geophysical Monograph Series, **13**, 18–36. AGU, Washington D.C.

BISWAS, N. N. & KNOPOFF, L. 1974. The structure of the upper mantle under the United States from the dispersion of Rayleigh waves. *Geophysical Journal of the Royal Astronomical Society*, **36**, 515–539.

BOHNHOFF, M., MAKRIS, J., PAPANIKOLAOU, P. & STAVRAKAKIS, G. 2001. Crustal investigation of the Hellenic subduction zone using wide aperture seismic data. *Tectonophysics*, **343**, 239–262.

BOSCHI, L., EKSTRÖM, G. & KUSTOWSKI, B. 2004. Multiple resolution surface wave tomography: the Mediterranean basin. *Geophysical Journal International*, **157**, 293–304.

BOUROVA, E., KASSARAS, I., PEDERSEN, H. A., YANOVSKAYA, T., HATZFELD, D. & KIRATZI, A. 2005. Constraints on absolute S velocities beneath the Aegean Sea from surface wave analysis. *Geophysical Journal International*, **160**, 1006–1019.

BROOKS, M. & KIRIAKIDIS, L. 1986. Subsidence of the North Aegean Trough: an alternative view. *Journal of the Geological Society, London*, **143**, 23–27.

CALCAGNILE, G. & PANZA, G. F. 1980. The main characteristics of the lithosphere–asthenosphere system in Italy and surrounding regions. *Pure and Applied Geophysics*, **119**, 865–879.

CALCAGNILE, G., D'INGEO, F., FARRUGIA, P. & PANZA, G. F. 1982. The lithosphere in the central–eastern Mediterranean area. *Pure and Applied Geophysics*, **120**, 389–406.

CANITEZ, N. & TOKSOZ, M. N. 1971. Focal mechanism and source depth of earthquakes from body and surface wave data. *Bulletin of the Seismological Society of America*, **61**, 1369–1379.

CAPUTO, M., PANZA, G. F. & POSTPISCHL, D. 1970. Deep structure of the Mediterranean basin. *Journal of Geophysical Research*, **75**, 4919–4923.

CHAILAS, S., HIPKIN, R. G. & LAGIOS, E. 1993. Isostatic studies in the Hellenides. *In*: 2nd *Congress of the Hellenic Geophysical Union, 5–7 May, Florina, Greece*, **2**, 492–504.

CHRISTODOULOU, A. & HATZFELD, D. 1988. Three-dimensional crustal and upper mantle structure beneath Chalkidiki (northern Greece). *Earth and Planetary Science Letters*, **88**, 153–168.

CLEMENT, C., SACHPAZI, M., CHARVIS, P., GRAINDERGE, D., LAIGLE, M., HIRN, A. & ZAFIROPOULOS, G. 2004. Reflection–refraction seismics in the Gulf of Corinth: hints at deep structure and control of the deep marine basin. *Tectonophysics*, **391**, 97–108.

DELIBASIS, N., MAKRIS, J. & DRAKOPOULOS, J. 1988. Seismic investigation of the crust and the upper mantle in western Greece. *Annales Géologiques de Pays Helléniques*, **33**, 69–83.

DITMAR, P. G. & YANOVSKAYA, T. B. 1987. A generalization of the Backus–Gilbert method for estimation of lateral variations of surface wave velocity. *Physics of the Solid Earth, Izvestia Academy of Sciences, USSR*, **23**, 470–477.

DRAKATOS, G. 1989. *Seismic tomography—determination of high and low velocity zones beneath Greece and surrounding regions.* PhD thesis, University of Athens. XXIII, **3**, 157–172.

DRAKATOS, G. & DRAKOPOULOS, J. 1991. 3-D velocity structure beneath the crust and upper mantle of the Aegean sea region. *Pure and Applied Geophysics*, **135**, 401–420.

DRAKATOS, G., LATOUSSAKIS, J., STAVRAKAKIS, G., PAPANASTASIOU, D. & DRAKOPOULOS, J. 1989. 3-Dimensional velocity structure of the north–central Greece from inversion of travel times. *In*: *3rd Congress of the Geological Society of Greece.* Geological Society of Greece, Athens XXIII, **3**, 157–172.

ENDRUN, B., CERANNA, L., MEIER, T., RISCHE, M., BOHNHOFF, M. & HARJES, H.-P. 2005. Structural properties of the Hellenic subduction zone derived from receiver functions and surface wave dispersion. *Geophysical Research Abstracts*, **7**, 7123.

ENDRUN, B., MEIER, T., LEBEDEV, S., BOHNHOFF, M. & HARJES, H.-P. 2006. Constraints on S-velocity, radial and azimuthal anisotropy in the Aegean region from surface wave dispersion, *Geophysical Research Abstracts*, **8**, 7830.

FLEISCHER, U. 1964. Schwerestorungen im ostlichen Mittelmeer: nach Messungen mit einem Askania-Seegravimeter. *Deutsche Hydrographische Zeitschrift* **17**, 153.

FYTIKAS, M., INNOCENTI, F., MANETTI, P., MAZZUOLI, R., PECCERILLO, A. & VILLARI, L. 1984. Tertiary to Quaternary evolution of the volcanism in the Aegean region. *In*: DIXON, J. E. & ROBERTSON, A. H. F. (eds) *The Geological Evolution of the Eastern Mediterranean*. Geological Society, London, Special Publications, **17**, 687–699.

GEORGALAS, G. 1962. *Catalogue of the Active Volcanoes and Solfatara Fields in Greece, Part 12*. International Association of Volcanology, Rome.

GOK, R., TURKELLI, N., SANDVOL, E., SEBER, D. & BARAZANGI, M. 2000. Regional wave propagation in Turkey and surrounding regions. *Geophysical Research Letters*, **27**, 429–432.

HASHIDA, T., STAVRAKAKIS, G. & SHIMAZAKI, K. 1988. Three-dimensional seismic attenuation beneath the Aegean region and its tectonic implication. *Tectonophysics*, **145**, 43–54.

HATZFELD, D., KARAGIANNI, E., KASSARAS, I., *ET AL*. 2001. Shear wave anisotropy in the upper mantle beneath the Aegean related to internal deformation. *Journal of Geophysical Research*, **106**, 30737.

HURTIG, E., CERMAK, V., HAENEL, R. & ZUI, V. 1991. *Geothermal Atlas of Europe.* Hermann Haack, Gotha.

JACKSON, J. 1994. Active tectonics of the Aegean region. *Annual Review of Earth and Planetary Sciences*, **22**, 239–271.

JOBERT, N. & JOBERT, J. 1983. An application of the ray theory to the propagation of waves along a laterally heterogeneous spherical surface. *Geophysical Research Letters*, **10**, 1148–1151.

KALOGERAS, J. S. 1993. *A contribution of surface seismic waves in the study of the crust and upper mantle in the area of Greece*. PhD thesis, University of Athens.

KALOGERAS, J. S. & BURTON, P. W. 1996. Shear-wave velocity models from Rayleigh-wave dispersion in the broader Aegean area. *Geophysical Journal International*, **125**, 679–695.

KARAGIANNI, E. E., PANAGIOTOPOULOS, D. G., PANZA, G. F., *ET AL*. 2002. Rayleigh wave group velocity tomography in the Aegean area. *Tectonophysics*, **358**, 187–209.

KARAGIANNI, E. E., PAPAZACHOS, C. B., PANAGIOTOPOULOS, D. G., SUHADOLC, P., VUAN, A. & PANZA, G. F. 2005. Shear velocity structure in the Aegean area obtained by inversion of Rayleigh waves. *Geophysical Journal International*, **160**, 127–143.

KEILIS-BOROK, V. I. & YANOVSKAYA, T. B. 1967. Inverse problems of seismology. *Geophysical Journal of the Royal Astronomical Society*, **13**, 223–234.

KIRATZI, A. A., PAPADIMITRIOU, E. E. & PAPAZACHOS, B. C. 1987. A microearthquake survey in the Steno dam site in northwestern Greece. *Annales Geophysicae*, **5**, 161–166.

KIRIAKIDIS, L. G. 1988. The Vardar ophiolite: a continuous belt under the Axios basin sediments. *Geophysical Journal International*, **98**, 203–212.

KNOPOFF, L. 1964. A matrix method for elastic wave problems. *Bulletin of the Seismological Society of America*, **54**, 431–438.

KNOPOFF, L. 1972. Observation and inversion of surface wave dispersion. *Tectonophysics*, **13**, 497–519.

KURT, H., DEMIRBAG, E. & KUSCU, I. 1999. Investigation of the submarine active tectonism in the gulf of Gokova, southwest Anatolia–southeast Aegean Sea, by multi-channel seismic reflection data. *Tectonophysics*, **305**, 477–496.

LE PICHON, X. & ANGELIER, J. 1979. The Hellenic arc and trench system: a key to the neotectonic evolution of the eastern Mediterranean area. *Tectonophysics*, **60**, 1–42.

LEVSHIN, A. L., RATNIKOVA, L. I. & BERTEUSSEN, K. A. 1972. On a frequency–time analysis of oscillations. *Annales Geophysicae*, **28**, 211–218.

LEVSHIN, A. L., YANOVSKAYA, T. B., LANDER, A. V., BUKCHIN, B. G., BARMIN, M. P., RATNIKOVA, L. I. & ITS, E. N. 1989. Recording, identification and measurement of surface wave parameters. *In*: KEILIS-BOROK, V. I. (ed.) *Seismic Surface Waves in a Laterally Inhomogeneous Earth*. Kluwer, Dordrecht, 131–182.

LEVSHIN, A. L., RATNIKOVA, L. I. & BERGER, J. 1992. Peculiarities of surface-wave propagation across central Eurasia. *Bulletin of the Seismological Society of America*, **82**, 2464–2493.

LI, X., BOCK, G., VAFIDIS, A., *ET AL*. 2003. Receiver function study of the Hellenic subduction zone: imaging crustal thickness variations and the oceanic Moho of the descending African lithosphere. *Geophysical Journal International*, **155**, 733–748.

LIGDAS, C. N. & LEES, J. M. 1993. Seismic velocity constrains in the Thessaloniki and Chalkidiki areas (northern Greece) from a 3D tomographic study. *Tectonophysics*, **228**, 97–121.

LIGDAS, C. N. & MAIN, I. G. 1991. On the resolving power of tomographic images in the Aegean area. *Geophysical Journal International*, **107**, 197–203.

LIGDAS, C. N., MAIN, I. G. & ADAMS, R. D. 1990. 3D structure of the lithosphere in the Aegean Sea region. *Geophysical Journal International*, **102**, 219–229.

MAKRIS, J. 1973. Some geophysical aspects of the evolution of the Hellenides. *Bulletin of the Geological Society of Greece*, **10**, 206–213.

MAKRIS, J. A. 1976. A dynamic model of the Hellenic arc deduced from geophysical data. *Tectonophysics*, **36**, 339–346.

MAKRIS, J. A. 1977. *Geophysical Investigation of the Hellenides. Hamburger Geophysikalische Einzelschriften*, **34**, 124.

MAKRIS, J. A. 1978. The crust and upper mantle of the Aegean region from deep seismic soundings. *Tectonophysics*, **46**, 269–284.

MARQUERING, H. & SNIEDER, R. 1996. Shear-wave velocity structure beneath Europe, the northeastern Atlantic and western Asia from waveform inversions

including surface-wave mode coupling. *Geophysical Journal International*, **127**, 283–304.

MARTIN, L. 1987. *Structure et évolution récente de la Mer Egée*. Thèse de Doctorat, Université Paris-Sud.

MARTINEZ, M. D., LANA, X., CANAS, J. A., BADAL, J. & PUJADES, L. 2000. Shear-wave velocity tomography of the lithosphere–asthenosphere system beneath the Mediterranean area. *Physics of the Earth and Planetary Interiors*, **122**, 33–54.

MCKENZIE, D. P. 1970. The plate tectonics of the Mediterranean region. *Nature*, **226**, 239–243.

MCKENZIE, D. P. 1972. Active tectonics of the Mediterranean region. *Geophysical Journal of the Royal Astronomical Society*, **30**, 109–185.

MCKENZIE, D. P. 1978. Active–tectonics of the Alpine–Himalayan belt: the Aegean Sea and surrounding regions. *Geophysical Journal of the Royal Astronomical Society*, **55**, 217–254.

MCCLUSKY, S., BALASSANIAN, S., BARKA, A., *ET AL.* 2000. Global Positioning System constraints on plate kinematics and dynamics in the eastern Mediterranean and Caucasus. *Journal of Geophysical Research*, **105**, 5695–5719.

MEIER, T., DIETRICH, K., STOCKHERT, B. & HARJES, H.-P. 2004. One-dimensional models of shear wave velocity for the eastern Mediterranean obtained from the inversion of Rayleigh wave phase velocities and tectonic implications. *Geophysical Journal International*, **156**, 45–58.

MINDEVALLI, O. Y. & MITCHELL, B. J. 1989. Crustal structure and possible anisotropy in Turkey from seismic surface wave dispersion. *Geophysical Journal International*, **98**, 93–106.

MONTAGNER, J. P. & TANIMOTO, T. 1991. Global upper mantle tomography of seismic velocities and anisotropies. *Journal of Geophysical Research*, **96**, 20337–20351.

MUELLER, S. 1977. A new model of the continental crust. *In*: HEACOOK, J. G. (ed.) *The Earth's Crust: its Nature and Physical Properties*. Geophysical Monograph, American Geophysical Union, **20**, 289–317.

PANAGIOTOPOULOS, D. G. 1984. *Travel time curves and crustal structure in the southern Balkan region*. PhD thesis, University of Tessaloniki.

PANAGIOTOPOULOS, D. G. & PAPAZACHOS, B. C. 1985. Travel times of Pn waves in the Aegean and surrounding area. *Geophysical Journal of the Royal Astronomical Society*, **80**, 165–176.

PANZA, G. F. 1981. The resolving power of seismic surface waves with respect to crust and upper mantle structural models. *In*: CASSINIS, R. (ed.) *The Solution of the Inverse Problem in Geophysical Interpretation*. Plenum, New York, 39–77.

PANZA, G. F., PONTEVIVO, A., SARAÓ, A., AOUDIA, A. & PECCERILLO, A. 2004. Structure of the lithosphere–asthenosphere and volcanism in the Tyrrhenian Sea and surroundings. *Memorie del Servizio Geologico*, **XLIV**, 29–56.

PAPAZACHOS, B. C. 1969. Phase velocities of Rayleigh waves in southeastern Europe and eastern Mediterranean Sea. *Pure and Applied Geophysics*, **75**, 47–55.

PAPAZACHOS, B. C. & COMNINAKIS, P. E. 1969. Geophysical features of the Greek islands Arc and Eastern Mediterranean Ridge. *Comptes Rendus Séance Conference Réunie Madrid*, **16**, 74–75.

PAPAZACHOS, B. C. & COMNINAKIS, P. E. 1971. Geophysical and tectonic features of the Aegean arc. *Journal of Geophysical Research*, **76**, 8517–8533.

PAPAZACHOS, B. C. & DELIBASIS, N. D., 1969. Tectonic stress field and seismic faulting in the area of Greece. *Tectonophysics*, **7**, 231–255.

PAPAZACHOS, B. C. & PAPAZACHOU, C. B. 1997. *The Earthquakes of Greece*. Ziti, Thessaloniki.

PAPAZACHOS, B. C., POLATOU, M. & MANDALOS, N. 1967. Dispersion of surface waves recorded in Athens. *Pure and Applied Geophysics*, **67**, 95–106.

PAPAZACHOS, B. C., KIRATZI, A., HATZIDIMITRIOU, P. & ROCCA, A. 1984. Seismic faults in the Aegean area. *Tectonophysics*, **106**, 71–85.

PAPAZACHOS, B. C., PAPADIMITRIOU, E. E., KIRATZI, A. A., PAPAZACHOS, C. B. & LOUVARI, E. K. 1998. Fault plane solutions in the Aegean Sea and the surrounding area and their tectonic implications. *Bolletino di Geofisica Teorica ed Applicata*, **39**, 199–218.

PAPAZACHOS, C. B. 1993. Determination of crustal thickness by inversion of travel times with an application in the Aegean area. *In*: *2nd Congress of the Hellenic Geophysical Union, 5–7 May, Florina, Greece,* **3**, 483–491.

PAPAZACHOS, C. B. 1994. *Structure of the crust and upper mantle in SE Europe by inversion of seismic and gravimetric data*. PhD thesis, University of Thessaloniki. [in Greek]

PAPAZACHOS, C. B. 1998. Crustal and upper mantle P and S velocity structure of the Serbomacedonian massif (Northern Greece). *Geophysical Research Letters*, **134**, 25–39.

PAPAZACHOS, C. B. & NOLET, G. 1997. P and S deep structure of the Hellenic area obtained by robust nonlinear inversion of travel times. *Journal of Geophysical Research*, **102**, 8349–8367.

PAPAZACHOS, C. B., HATZIDIMITRIOU, P. M., PANAGIOTOPOULOS, D. G. & TSOKAS, G. N. 1995. Tomography of the crust and upper mantle in southeast Europe. *Journal of Geophysical Research*, **100**, 405–422.

PASYANOS, M. E., WALTER, W. R. & HAZLERT, S. E. 2001. A surface wave dispersion study of the Middle East and North Africa for monitoring the comprehensive nuclear-test-ban treaty. *Pure and Applied Geophysics*, **158**, 1445–1474.

PAYO, G. 1967. Crustal structure of the Mediterranean Sea by surface waves. Part I, Group velocity. *Bulletin of the Seismological Society of America*, **57**, 151–172.

PAYO, G. 1969. Crustal structure of the Mediterranean sea by surface waves. Part II, Phase velocity and travel times. *Bulletin of the Seismological Society of America*, **59**, 23–42.

PLOMEROVA, J., BABUSKA, V., PUJDUSAK, P., HATZIDIMITRIOU, P., PANAGIOTOPOULOS, D., KALOGERAS, J. & TASSOS, S. 1989. Seismicity of the Aegean and surrounding areas in relation to topography of the lithosphere–asthenosphere transition. *In*: *Proceedings of the 4th International Symposium on Analysis Seismicity and Seismic Risk, Bechyne, Czechoslovakia, 4–9 September*, 209–215.

PONTEVIVO, A. & PANZA, G. F. 2002. Group velocity tomography and regionalization in Italy and bordering areas. *Physics of the Earth and Planetary Interiors*, **134**, 1–15.

RAYKOVA, R. B. & NIKOLOVA, S. B. 2000. Shear wave velocity models of the Earth's crust and uppermost mantle from the Rayleigh waves in Balkan Peninsula and adjacent areas. *Bulgarian Geophysical Journal*, **26**, 11–27.

RAYKOVA, R. B. & NIKOLOVA, S. B. 2003. Anisotropy in the Earth's crust and uppermost mantle in southeastern Europe obtained from the Rayleigh and Love surface waves. *Journal of Applied Geophysics*, **54**, 247–256.

ROUSSOS, N. 1994. Stratigraphy and paleogeographic evolution of the Paleogene Molassic basins of the North Aegean area. *Bulletin of the Geological Society of Greece*, **XXX**, 275–294.

SAATCILAR, R., ERGINTAV, S., DEMIRBAG, E. & INAN, S. 1999. Character of active faulting in the North Aegean Sea. *Marine Geology*, **160**, 339–353.

SAUNDERS, P., PRIESTLEY, K. & TAYMAZ, T. 1998. Variations in the crustal structure beneath western Turkey. *Geophysical Journal International*, **134**, 373–389.

SCHWAB, F. A. & KNOPOFF, L. 1972. Fast surface wave and free mode computations. *In*: BOLT, B. A (ed.) *Methods in Computational Physics*. Academic Press, New York, 86–180.

SCHWAB, F. A., NAKANISHI, K., CUSCITO, M., PANZA, G. F. & LIANG, G. 1984. Surface-wave computations and the synthesis of theoretical seismograms at high frequencies, *Bulletin of the Seismological Society of America*, **74**, 1555–1578.

SCORDILIS, E. M., KARAKAISIS, G. F., KARACOSTAS, B. G., PANAGIOTOPOULOS, D. G., COMNINAKIS, P. E. & PAPAZACHOS, B. C. 1985. Evidence for transforming faulting in the Ionian Sea: the Cefalonia island earthquake sequence of 1983. *Pure and Applied Geophysics*, **123**, 388–397.

SPAKMAN, W. 1986. Subduction beneath Eurasia in connection with the Mesozoic Tethys. *Geologie en Mijnbouw*, **65**, 145–153.

SPAKMAN, W., WORTEL, M. J. R. & VLAAR, N. J. 1988. The Hellenic subduction zone: atomographic image and its dynamic implications. *Geophysical Research Letters*, **15**, 60–63.

SPAKMAN, W., VAN DER LEE, S. & VAN DER HILST, R. D. 1993. Travel-time tomography of the European–Mediterranean mantle down to 1400 km. *Physics of the Earth and Planetary Interiors*, **79**, 3–74.

TAYMAZ, T. 1996. S–P-wave traveltime residuals from earthquakes and lateral inhomogeneity in the upper mantle beneath the Aegean and the Hellenic Trench near Crete. *Geophysical Journal International*, **127**, 545–558.

TAYMAZ, T., JACKSON, J. & MCKENZIE, D. 1991. Active tectonics of the north central Aegean Sea. *Geophysical Journal International*, **106**, 433–490.

TIBERI, C., LYON-CAEN, H, HATZFELD, D., *ET AL.* 2000. Crustal and upper mantle structure beneath the Corinth rift (Greece) from a teleseismic tomography study. *Journal of Geophysical Research*, **105**, 28159–28171.

TIREL, C., GUEYDAN, F., TIBERI, C. & BRUN, J.-P. 2004. Aegean crustal thickness inferred from gravity inversion. Geodynamical implications. *Earth and Planetary Science Letters*, **228**, 267–280.

TSOKAS, G. N. & HANSEN, R. O. 1997. Study of the crustal thickness and the subducting lithosphere in Greece from gravity data. *Journal of Geophysical Research*, **102**, 20585–20597.

URBAN, L., CICHOWICZ, A. & VACCARI, F. 1993. Computation of analytical partial derivatives of phase and group velocities for Rayleigh waves with respect to structural parameters. *Studia Geophysica et Geodaetica*, **37**, 14–36.

VALYUS, V. P. 1968. Determining seismic profiles from a set of observations. *Vychislitelnaya Seismologiya*, **4**, 3–14. [in Russian]. (English translation in: KELLIS-BOROK, V. I. (ed.) *Computational Seismology*. Consultants Bureau, New York, 1972, 114–118.)

VOGT, P. & HIGGS, P. 1969. An aeromagnetic survey of the eastern Mediterranean Sea and its interpretation. *Earth and Planetary Science Letters*, **5**, 439–448.

VOULGARIS, N. 1991. *Investigation of the crustal structure in western Greece (Zakinthos–NW Peloponessus area)*. PhD thesis, University of Athens. [in Greek]

YANOVSKAYA, T. B. 1982. Distribution of surface wave group velocities in the North Atlantic. *Izvestiya Akademi Nauk SSSR, Fizika Zemli*, **2**, 3–11.

YANOVSKAYA, T. B. 1997. Resolution estimation in the problems of seismic ray tomography. *Izvestia, Physics of the Solid Earth*, **33**, 762–765.

YANOVSKAYA, T. B. & DITMAR, P. G. 1990. Smoothness criteria in surface wave tomography. *Geophysical Journal International*, **102**, 63–72.

YANOVSKAYA, T. B., KIZIMA, E. S. & ANTOMOVA, L. M. 1998. Structure of the crust in the Black Sea and adjoining regions from surface wave data. *Journal of Seismology*, **2**, 303–316.

YANOVSKAYA, T. B., ANTOMOVA, L. M. & KOZHEVNIKOV, V. M. 2000. Lateral variations of the upper mantle structure in Eurasia from group velocities of surface waves. *Physics of the Earth and Planetary Interiors*, **122**, 19–32.

ZELIMER, G. F. 1998. *Petrogenetic processes and their timescales beneath Santorini, Aegean Volcanic Arc, Greece*. PhD thesis, The Open University, Milton Keynes.

ZHAO, D., CHRISTENSEN, D. & PULPAN, H. 1995. Tomographic imaging of the Alaska subduction zone. *Journal of Geophysical Research*, **100**, 6487–6504.

ZHAO, D., XU, Y., WIENS, D. A., DORMAN, L., HILDEBRAND, J. & WEBB, S. 1997. Depth extent of the Lau back-arc spreading center and its relation to subduction processes. *Science*, **278**, 254–257.